Earthq Eng & Eng Vib (2019) 18: 845-869 **DOI**: https://doi.org/10.1007/s11803-019-0539-0

Behavior of ductile steel X-braced RC frames in seismic zones

Eber Alberto Godínez-Domínguez[1†] and Arturo Tena-Colunga[2†]

1. *Facultad de Ingeniería, Universidad Autónoma de Chiapas, Tuxtla Gutiérrez 29050, Mexico*
2. *Departamento de Materiales, Universidad Autónoma Metropolitana, México City 02200, Mexico*

Abstract: A satisfactory ductile performance of moment-resisting reinforced concrete concentric braced frame structures (RC-MRCBFs) is not warranted by only following the provisions proposed in Mexico's Federal District Code (MFDC-04). The nonlinear behavior of low to medium rise ductile RC-MRCBFs using steel X-bracing susceptible to buckling is evaluated in this study. The height of the studied structures ranges from 4 to 20 stories and they were located for design in the lake-bed zone of Mexico City. The design of RC-MRCBFs was carried out considering variable contribution of the two main lines of defense of the dual system (RC columns and steel braces). In order to observe the principal elements responsible for dissipating the earthquake input energy, yielding mappings for different load-steps were obtained using both nonlinear static and dynamic analyses. Some design parameters currently proposed in MFDC-04 as global ductility capacities, overstrength reduction factors and story drifts corresponding to different limit states were assessed as a function of both the considered shear strength and slenderness ratios for the studied RC-MRCBFs using pushover analyses. Additionally, envelopes of response maxima of dynamic parameters were obtained from the story and global hysteresis curves. Finally, a brief discussion regarding residual drifts, residual drift ratios, mappings of residual deformations in steel braces and residual rotations in RC beams and columns is presented. From the analysis of the obtained results, it is concluded that when a suitable design criterion is considered, good structural behavior of RC-MRCBFs with steel-X bracing can be obtained. It is also observed that the shear strength balance has an impact in the height-wise distribution of residual drifts, and an important "shake-down" effect is obtained for all cases. There is a need to improve design parameters currently proposed in MFDC to promote an adequate seismic performance of RC-MRCBFs.

Keywords: RC braced-frames; seismic design; nonlinear dynamic analyses; steel-X bracing; overstrength; collapse mechanism; story drifts; residual drifts

1 Introduction

Often, during the design of a new low or medium-rise flexural building in a zone of moderate to high seismic risk and hazard, structural engineers usually use concrete or masonry shear walls to increase the in-plane shear stiffness and strength of RC-framed buildings subjected to strong earthquake loading, whereas the use of steel bracing is more often in steel frames.

As a consequence of strong earthquakes observed in Mexico and around the world, RC buildings have been seriously damaged as a result of a number of different factors (Borja-Navarrete *et al.*, 1986; Aschheim *et al*., 2000; Sharmaa *et al*., 2011), such as design and/or construction process errors, as well as inadequate seismic hazard assessments. These factors were evident once again during the reconnaissance of severely damaged buildings that was made after the occurrence of the most recent strong earthquakes in Mexico on September 7 (M_w = 8.2) and 19 (M_w = 7.1), 2017. There are several suitable techniques for seismic rehabilitation that have been used around the world (e.g., steel cables, carbon fibers, concrete shear walls, concrete jacketing, isolation systems, energy dissipation devices, steel bracing). Over many years, due to the improvement observed in the structural behavior of earthquake-damaged buildings (Del Valle, 1980; Del Valle *et al*., 1988; Foutch *et al*., 1989; Downs *et al.*, 1991; Badoux and Jirsa, 1990; Bush *et al*., 1991; Tagawa *et al.*, 1992; Masri and Goel, 1996; Tena-Colunga *et al*., 1996; Ghobarah and Abou-Elfath, 2001; Osman *et al*., 2006; Xiao *et al.,* 2011; Kadid and Yahiaoui, 2011; Liu *et al*., 2012; Tong *et al*., 2012; Zhang *et al.*, 2013; Ju *et al*., 2014), one of the most popular retrofitting strategies to increase the lateral stiffness and strength of RC structures is based on the use of steel braces considering different layouts in plan and elevation. In fact, some studies have shown that the use of different bracing configurations could highly influence, among other structural parameters, the lateral

Correspondence to: Eber Alberto Godínez-Domínguez, Facultad de Ingeniería, Universidad Autónoma de Chiapas, Tuxtla Gutiérrez 29050, Mexico
Tel: +52-019616150322; Fax: (011) (+52-961) 61505-27
E-mail: eber.godinez@unach.mx
†Professor

Received October 18, 2017; **Accepted** March 21, 2018

strength and lateral stiffness, the forces transferred to joints directly connected to steel bracings as well as the assessment of global design parameters (Maheri *et al.*, 2003; Faella *et al.*, 2014). Thus, bracing configuration must be carefully evaluated during a design process in order to obtain a suitable seismic response and also, for the retrofitting cases, to try to avoid significant retrofitting costs due to the unfavorable configuration of bracings and their effects in terms of forces transmitted to both existing members and foundations (Faella *et al.*, 2014).

As an alternative to the use of traditional braces (susceptible to buckling), new or existing RC buildings could be designed or retrofitted by using braces with energy dissipation devices (EDD), such as buckling restrained braces, BRBs or other EDD mounted on steel braces. By using this strategy, not only the lateral stiffness and lateral force capacity is increased, but also the energy dissipation capacity. It has also been shown that it helps avoid drift concentrations at few stories and promotes a favorable and dissipative collapse mechanism (e.g., Tena-Colunga *et al.*, 1996; Ghaffarzadeh and Maheri, 2006; Khampanit *et al.*, 2014; Tena-Colunga and Nangullasmú-Hernández, 2015; Barbagallo *et al*., 2017; Aval *et al*., 2017). Many analytical and experimental research studies have shown the suitability of such devices to improve the seismic behavior of RC structures, and also their advantages to minimize interference with the functions and aesthetics in the case of damage to existing buildings, or buildings that were designed according to old seismic standards that have structural deficiencies that need to be corrected (e.g., Martínez-Romero, 1993; Tena-Colunga *et al.*, 1996; Della Corte *et al*., 2015; Barbagallo *et al*., 2017; Almeida *et al*., 2017; Qu *et al*., 2017). Note that although it has been shown that EDD mounted on steel bracing and BRBs are suitable energy dissipation devices for the original design and retrofit of structures, in Mexico, one of the main reasons for the limited use of such devices for new design or the seismic retrofitting of RC and steel buildings is directly related to the initial investment (Tena-Colunga, 2007). Thus, traditional braces are still widely used in most cases.

As a progressive process on the use of traditional steel bracing systems, and given the adequate seismic structural performance observed in the retrofitted RC buildings during the registered earthquakes in Mexico (Del Valle *et al*., 1988; Foutch *et al*., 1989; Downs *et al.*, 1991; Tena-Colunga *et al.*, 1996) and around the world (Kawamata and Onhuma, 1980; Nateghi, 1995), this dual system, in which the structural response is highly influenced by the slenderness ratio of the steel bracing elements, is currently considered as a suitable alternative for the seismic design of new buildings. Note that in MFDC, the design of RC-MRCBFs has been allowed over the past three decades, even considering the possibility of a ductile behavior.

Since the late 1990's, some studies have been developed focused on proposing some specific design parameters, as well as on developing general criteria for the design of new RC-MRCBFs considering some steel bracing configurations (Maheri and Sahebi, 1997; Maheri and Akbari, 2003; Maheri and Hadjipour, 2003; Youssef *et al*., 2007; Maheri and Ghaffarzadeh, 2008; Godínez-Domínguez and Tena-Colunga, 2010; Godínez-Domínguez *et al.*, 2012; Maheri and Yazdani, 2016; Godínez-Domínguez and Tena-Colunga, 2016; Eskandari *et al.*, 2017; Qiao *et al*., 2017).

In a previous research study (Godínez-Domínguez and Tena-Colunga, 2010 and 2016; Godínez-Domínguez *et al*., 2012), the nonlinear static and dynamic behavior of RC-MRCBFs using steel-inverted V bracing was studied. The main objective of these previous studies was focused on developing some guidelines for the new design of braced RC buildings. However, the use of RC-MRCBFs with steel-X bracing has been popular and dominant for years in Mexico (Del Valle *et al.*, 1988; Foutch *et al.*, 1989; Downs *et al*., 1991; Tena-Colunga *et al.*, 1996). In fact, it seems that its use is frequent in other nations as well (Nateghi, 1995; Abou-Elfath and Ghobarah, 2000; Maheri and Akbari, 2003; Maheri *et al.*, 2003; Youssef *et al*., 2007; Maheri and Ghaffarzadeh, 2008; El-Sokkary and Galal, 2009; Ju *et al.*, 2014). Therefore, the study of RC-MRCBFs using steel-X bracing with ductile behavior allows to complete the study of the two more common bracing arrangements used in Mexico, and perhaps worldwide.

This study is focused on the study of the nonlinear seismic behavior of low to medium rise RC-MRCBFs structures using steel-X bracing, located in high seismic hazard zones. One of the main purposes is to show that if suitable design procedures are employed, it is possible to perform the seismic design of new ductile RC-MRCBFs of low and medium height, achieving collapse mechanisms congruent to the collapse prevention philosophy of MFDC. Also, some design parameters, as global deformation capacities, overstrength reduction factors and story drifts corresponding to different limit states are evaluated as a function of shear strength ratios between the steel X-bracing system and the columns of the RC moment frame, as well as the building height. Their nonlinear dynamic behavior is also evaluated by using several artificial records. Some useful peak and average (average of peak responses for all the studied records) dynamic parameters are obtained from the story and global hysteresis curves. Finally, a brief discussion about residual drifts, residual drift ratios, mappings of residual deformations in steel braces and residual rotations in RC beams and columns is presented.

2 Design of steel-X braced RC frames

2.1 Design requirements for ductile RC-MRCBFS in MFDC

The design criteria considered in the seismic guidelines of Mexico's Federal District Code (NTCS-04,

2004) are based upon the consideration that seismic forces should be resisted by the two main lines of defense of the dual system (RC columns and steel braces), as shown in Fig. 1. In addition, for ductile behavior, opposite to what it is currently specified for non-ductile buildings, it is not allowed that the steel bracing system represents the main line of defense of the dual system under lateral loading. Thus, the contribution of the bracing system to the lateral shear strength must be limited up to half of the total lateral shear strength of the dual system. Therefore, it is important to study the effect of the above recommendation (shear strength balance between the two main components) on the structural performance of RC-MRCBFs when steel-X bracing is used.

2.2 Geometry and characteristics of the dual systems

As previously done for steel-inverted V braced frames, 30 regular X-braced frame models (4, 8, 12, 16 and 20 stories) were designed for the lake bed zone conditions (soft soils) of Mexico City. The selected geometry of the dual systems under study is shown in Fig. 2. In all cases, ductile behavior is considered, using the maximum NTCS-04 global ductility-related modification factor $Q = 4$. Note that in Mexican codes, the seismic response modification factor is named Q (and is similar to the C_d factor in the most recent U.S. codes), and it can adopt the following values: 1.0, 1.5, 2.0, 3.0 and 4.0. The Q factor used is a function of both the selected structural system and the detail used in the design and construction of the sections and members that make up the earthquake-resistant system (e.g., minimum dimension of cross sections, maximum section aspect ratios, minimum diameter and distribution of the transversal and longitudinal steel reinforcement over the members, etc.). The Q factors of Mexican codes account primarily for displacement ductility, redundancy and overstrength. A comprehensive description of global design parameters and notation for the Mexican codes (Q, Q' and R) and their relation and comparison with the terminology used in U.S. codes (C_d, R and Ω_0) is available elsewhere (Tena-Colunga, 1999; Tena-Colunga *et al.*, 2009; Godínez-Domínguez *et al*., 2012).

Structural properties used for the design of reinforced concrete and steel members are summarized in Table 1, where f'_c and E_c are the compressive strength and the elastic modulus for the concrete, f_y is the yielding stress for longitudinal and transverse steel reinforcement, and E_s and f_{ys} are the elastic modulus and the yielding stress for the steel. In all cases, the bracing members were designed using A36 steel.

As usually done in design and construction practice in Mexico, cross sections for all the structural members were changed at certain specified number of stories, according to the building height. In all cases, at the time of defining typical cross sections, symmetric reinforcement in plan is provided to minimize potential asymmetric strength (in

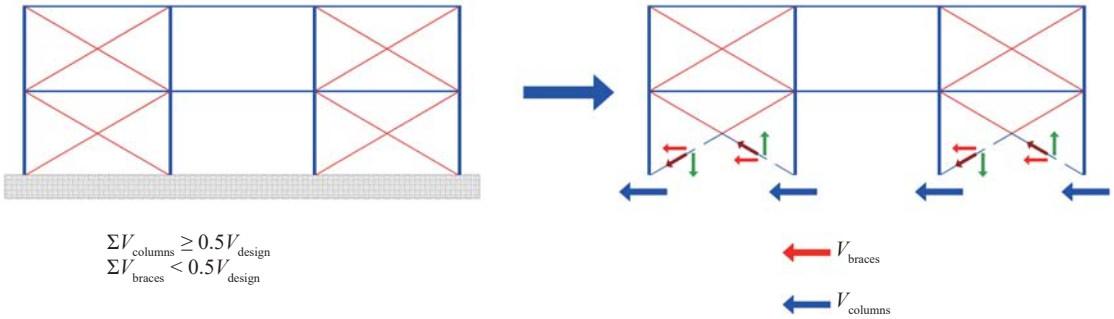

Fig. 1 Shear resistance mechanisms in RC-MRCBFs according to MFDC-04

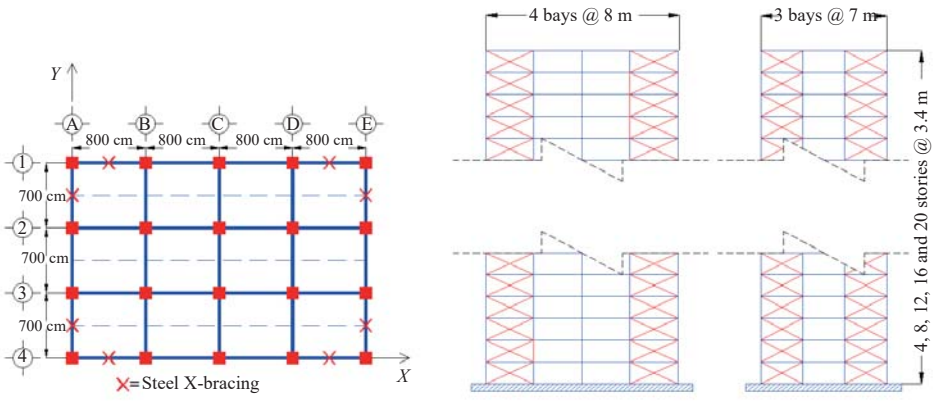

(a) Floor plan (b) Frame elevation in X and Y direction

Fig. 2 Geometry of the dual systems under study

Table 1 Material properties used for the design of RC and steel members

Building height	Concrete member properties			Steel member properties	
	f_c', MPa (kgf/cm^2 or psi)	E_c, MPa (kgf/cm^2)	f_y, MPa (kgf/cm^2 or psi)	f_{ys}, MPa (kgf/cm^2 or psi)	E_s, MPa (kgf/cm^2 or psi)
4 to 16-story models	24.53 (250 or 3,550)	$4400\sqrt{f_c'}$ ($14000\sqrt{f_c'}$)	412 (4,200 or 60)	248 (2530 or 36)	210 (2,100,000 or 147.84)
20-story models	34.34 (350 or 4,970)	$4400\sqrt{f_c'}$ ($14000\sqrt{f_c'}$)	412 (4,200 or 60)	248 (2530 or 36)	210 (2,100,000 or 147.84)

theory, the provided strength is symmetric). Also, in order to try to avoid stiffness irregularities along the height, cross sections of RC members are changed at different heights, and cross sections of the steel bracing members are changed at stories different from the ones selected for the RC members (Fig. 3).

Since the structural behavior of dual systems is highly influenced by the shear strength balance between the frame and the braces (Maheri and Akbari, 2003; Godínez-Domínguez and Tena-Colunga, 2010; Tong *et al*., 2012), models where 25%, 50% and 75% of the lateral shear strength is provided by the RC frame were considered for each building height.

2.3 Design methodology

The capacity design methodology used for the seismic design of the steel-X braced frames is based on the results of previous studies on steel-inverted V braced frames (Godínez-Domínguez and Tena-Colunga, 2010; Godínez-Domínguez *et al*., 2012). The sequence for designing resisting elements is explicitly taken into account in the proposed methodology. Therefore, earthquake-resistant members were designed from the weakest (steel braces) to the strongest (RC beams and RC columns). Finally, joint areas and connections between RC and steel members are considered. The proposed design methodology has also been recently used by Eskandari *et al.* (2017) for the study of the nonlinear behavior of dual reinforced concrete diagonal steel braced systems under far- and near-fault motions. Their models were able to achieve suitable structural behavior and collapse mechanisms, regardless of the type of the record.

The model identification key (ID), slenderness ratio (*H/L*), fundamental period (*T*) and modal mass are shown in Table 2 for all the studied models. The ID serves to

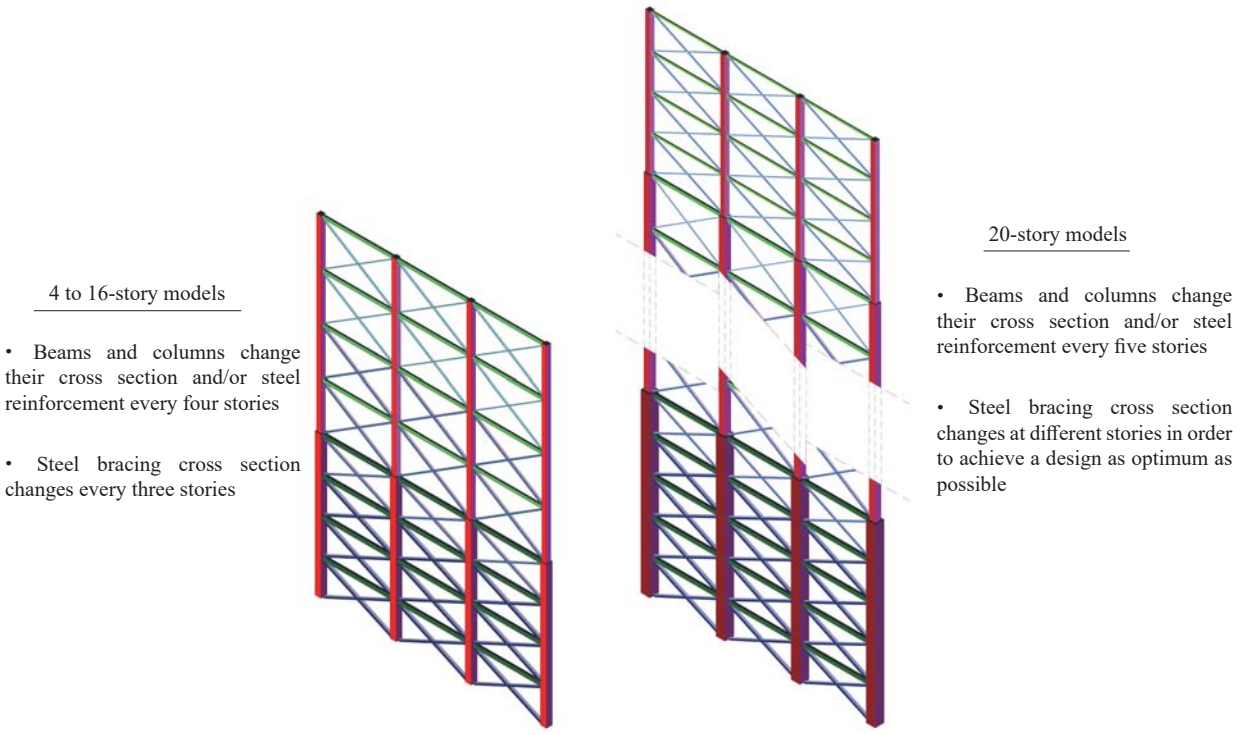

Fig. 3 Schematic representation of changes of cross sections for structural elements for the studied models

clearly identify each model and shear strength distribution between the components of the dual system (i.e., RC columns and steel-X braces). For example, the ID 16y25X is used to identify a sixteen story-model in the "*y*" direction (Fig. 2), where the shear strength contribution of the RC columns is 25% of the total (the considered values are 25%, 50% and 75%). Finally, the last letter indicates the bracing scheme used (in this case a letter X is used to indicate the use of steel-X bracing).

3 Nonlinear static analyses

As a first stage, nonlinear static analyses were carried out for all the designed RC-MRCBFs. These analyses can provide valuable information, such as global ductility capacities, overstrength reduction factors and story drifts corresponding to different limit states. Moreover, it is possible to observe the principal members that respond inelastically (e.g., height-wise distribution of possible damage related to different inter-story drifts).

3.1 Modeling assumptions and analyses control criterion

The strength and deformation capacities of reinforced concrete elements were obtained from their corresponding moment-curvature relationships (Wallace and Moehle, 1989). The effective flange of beams was considered in both stiffness and strength according to what is established in current reinforced concrete recommendations (NTCC-04, 2004) of Mexico City Code (MFDC-04, 2004).

In order to assess RC member capacities, the following assumptions are made. The modified Kent-Park model (Park *et al.*, 1982) was considered to assess overstrength due to concrete confinement. For the steel reinforcement, the stress-strain relationship used is the one developed for rebars produced in Mexico and based on the original Mander model (Andriono and Park, 1986), where $f_y = 450$ MPa (4,577 kgf/cm^2 or 65 ksi).

In order to obtain realistic results, pushover curves were limited according to the rotation capacity of the structural members (θ_p). For RC members, θ_p values were computed according to Eq. (1). Whereas, the methodology proposed by Kemp (1996) was used to compute the magnitude of the buckling length, which defines the failure of steel braces.

$$\theta_p = L_p\left(\varphi_u - \varphi_y\right) \tag{1}$$

where:

L_p = plastic hinge length, considered as $d/2$
d = effective depth of the member
φ_u = ultimate curvature
φ_y = yield curvature

3.2 Peak story drift envelopes

Subject buildings were rigorously designed, taking into account translational and rotational degrees of freedom and second-order (P-Δ) effects. Then, drifts were rigorously calculated taking into account both shear and flexural deformations; that is, in this paper, all the story and global drift curves are computed taking into account the total drift: the sum of shear and flexural drifts. Plotted peak story drifts depicted in Fig. 4 correspond to the following cases, when: (a) shear drifts are considered only, (b) flexural drifts are considered only, and (c) the total drift is considered. It is confirmed from the results shown in Fig. 4 that, as is well known, the importance of flexural drifts increases as the building height increases, and also, its impact is more notable as the contribution

Table 2 Dynamic characteristics of the investigated buildings

ID	H/L	T (s)	Modal mass (%)	ID	H/L	T (s)	Modal mass (%)
4x25X	0.43	0.283	85.90	12y25X	1.94	0.707	73.48
4x50X	0.43	0.311	85.45	12y50X	1.94	0.746	78.07
4x75X	0.43	0.278	85.60	12y75X	1.94	0.664	76.72
4y25X	0.65	0.231	85.36	16x25X	1.70	1.056	71.23
4y50X	0.65	0.250	85.74	16x50X	1.70	1.081	75.12
4y75X	0.65	0.230	84.75	16x75X	1.70	1.011	74.63
8x25X	0.85	0.484	78.16	16y25X	2.59	1.026	70.99
8x50X	0.85	0.556	80.31	16y50X	2.59	1.012	74.48
8x75X	0.85	0.533	79.44	16y75X	2.59	0.940	74.24
8y25X	1.30	0.438	77.28	20x25X	2.13	1.141	70.45
8y50X	1.30	0.484	79.39	20x50X	2.13	1.244	74.64
8y75X	1.30	0.434	79.29	20x75X	2.13	1.199	74.40
12x25X	1.28	0.769	74.43	20y25X	3.24	1.145	70.24
12x50X	1.28	0.849	77.00	20y50X	3.24	1.114	73.37
12x75X	1.28	0.768	76.97	20y75X	3.24	1.130	74.36

of the bracing system to the global stiffness and strength increases (12x25X and 20x25X models).

3.3 Capacity curves

Story and global capacity curves for some representative models are shown in Figs. 5 and 6 (8 and 16-story models, respectively). The results shown in these curves are representative of the medium-rise height building category that is most common in Mexico City. According to the findings derived from an experimental study on K-braced frames developed by Tagawa *et al.* (1992), the total capacity of the dual system can be computed as the sum of the individual components capacities (bracing system and RC frame), as indicated in Figs. 5 and 6.

From Figs. 5 and 6 it is possible to observe that a better structural behavior (an adequate height-wise distribution of damage) is achieved when the RC columns represent the main line of defense of the dual system (8x75X and 16x75X models) with regard to those models in which the bracing system is considered as the main line of defense (8x25X and 16x25X). The observed behavior in models where the RC columns represents the main line of defense of the dual system is desirable to get a more uniform distribution of the energy dissipation and, in fact, more energy dissipation capacity.

Opposite to the observations by Eskandari *et al.* (2017) for diagonal-steel RC braced frames, where the bracing systems were stiffer than RC frames when designed to have equal shear strength contribution, RC frames are stiffer for X-steel RC braced frames. This is because Eskandari *et al.* (2017) considered that braced frames had non-moment beam-to-column connections (were pinned).

It is also observed that the largest story drifts occur in the areas where there was a variation of the cross sections. As expected, and as shown in the following

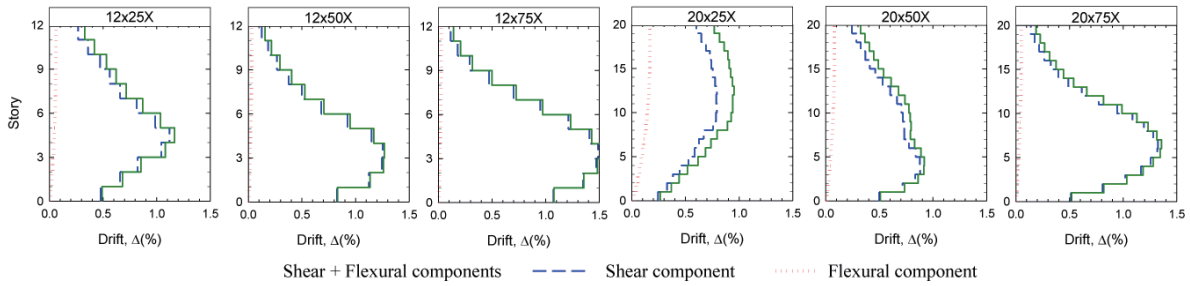

Fig. 4 Peak story drift envelopes accounting for both shear and flexural components

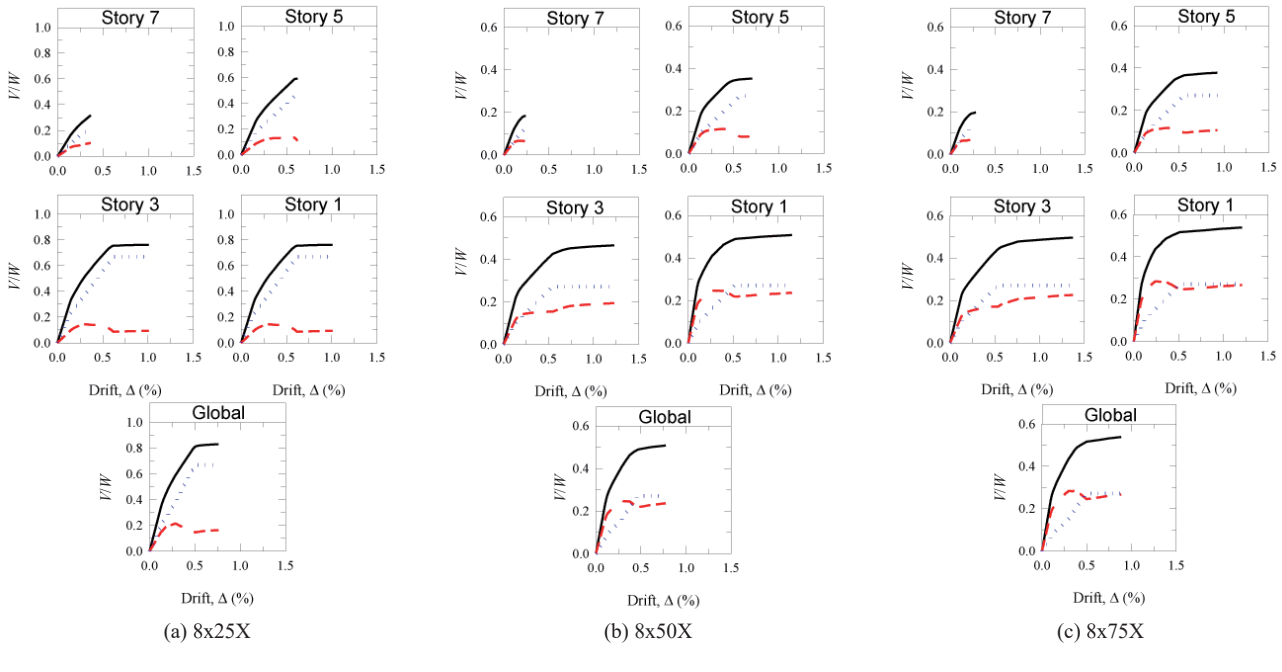

(a) 8x25X (b) 8x50X (c) 8x75X

Fig. 5 Story and global lateral shear-drift curves for the eight-story models

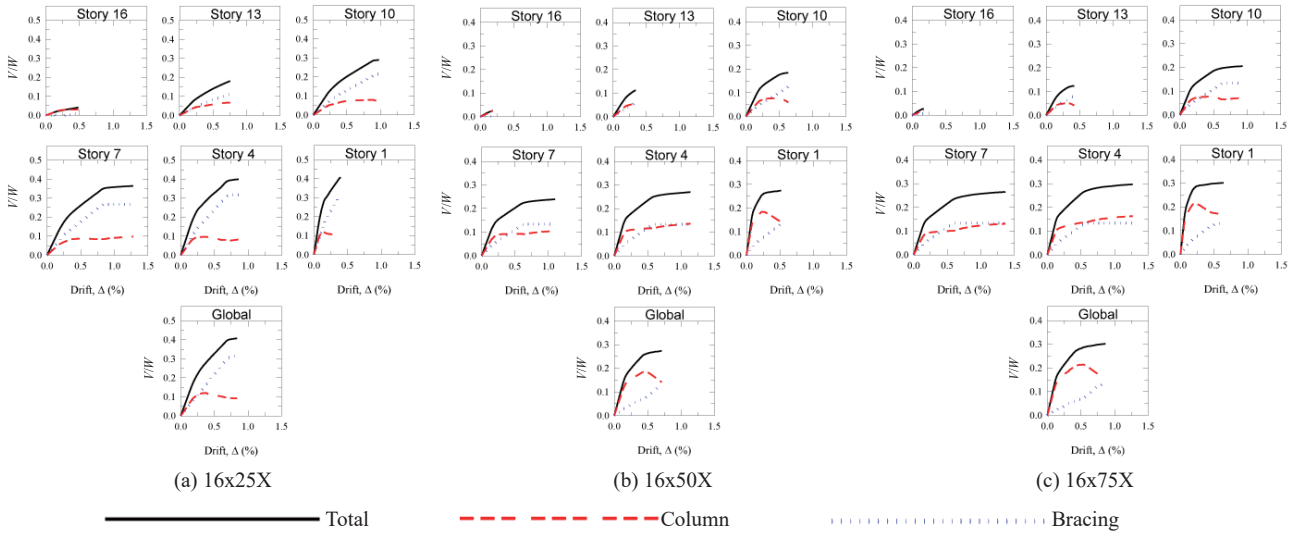

Fig. 6 Story and global lateral shear-drift curves for the sixteen-story models

sections, the members located in these areas are subjected to the greatest inelastic demands (this observation is also congruent with the nonlinear dynamic analyses results presented later).

3.4 Final collapse mechanisms

One of the most relevant issues during the study of the nonlinear behavior of a specific structural system is to assess the way in which the system could dissipate the input earthquake energy and verify if it is congruent with the corresponding failure mechanism supposed during the design stage. Due to the above, mappings of the sequences of yielding towards the formation of the failure mechanism were drawn at different stages along the pushover analysis.

In order to save space, Fig. 7 only shows yielding mappings associated to the step where the final collapse mechanism was achieved for some models in the *x* direction.

From the observation of the development of the formation of the failure mechanisms, it is concluded that strong-column, weak beam, weaker-brace collapse mechanisms can only be achieved in ductile models, where the RC columns of the moment frame represents the main line of defense of the dual system against earthquake forces (x50X and x75X models, Figs. 7(f)-(o)). For non-ductile models (x25X models, Figs. 7(a)-(e)), where the steel-X bracing system represents the main line of defense of the dual system, undesirable structural behavior could be developed, for example, the development of a weak-story mechanism or important plastic rotations demands in columns along the height of the buildings.

As structures become taller, it could be necessary to consider an additional requirement to try to avoid the development of inelastic hinge rotations in columns (Figs. 7(e), 7(j) and 7(o)). A suitable procedure could be based on the fact that as the shear strength percentage provided by the RC frame increases, the rotation demands in columns decreases. Then, a possible strategy could be based on an additional requirement where an increment in the shear strength contribution of the RC frame according to the specific characteristics of the geometry of the structures (e.g., slenderness ratio) is provided.

According to the results shown in this section, the guideline given in Mexican codes, in which the bracing system is not allowed to be the main line of defense of ductile dual systems is considered adequate. This is in agreement with previously reported studies for both steel-inverted V RC braced frames (Godínez-Domínguez and Tena-Colunga, 2010) and steel-diagonal RC braced frames (Eskandari *et al*., 2017).

3.5 Global ductility capacity (μ)

Structure inelastic deformation capacities ($\mu = \Delta/\Delta_y$) were obtained considering an equivalent energy criterion (i.e., the areas under the actual capacity curve and the equivalent bilinear idealized curve are equal, Newmark and Hall, 1982; FEMA-273, 1997). A clear tendency is observed in the results shown in Fig. 8: as the slenderness ratio increases, the peak global ductility decreases.

As observed from Figs. 7-8, only for ductile models, it is possible to achieve a structural performance with a stable collapse mechanism and global inelastic deformation capacities equal to or higher than the deformation demand used in the design stage ($\mu_{global} \geq Q = 4$). These analytical results are also in agreement with those previously reported for inverted-V braced structures (Godínez-Domínguez and Tena-Colunga, 2010 and 2016) and again support the criterion currently established in Mexican seismic guidelines regarding limiting the shear strength contribution of the bracing system for the ductile design of steel-braced RC structures up to half of the total lateral shear strength.

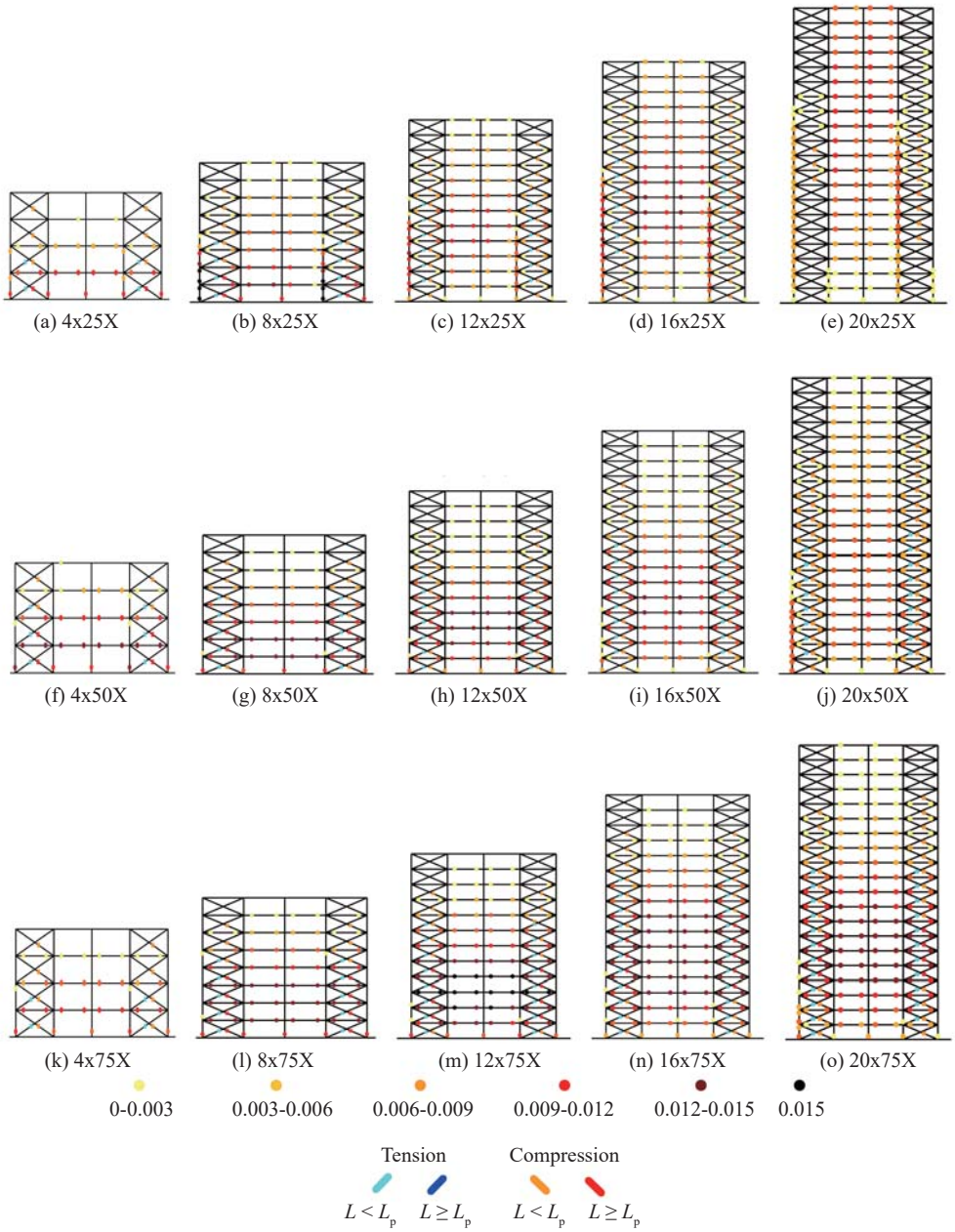

Fig. 7 Collapse mechanisms for models designed considering different lateral shear strength balance between the frames and the bracing system

4 Evaluation of some key design parameters

From a code-oriented viewpoint, global design parameters are needed for a ductile design of the studied braced RC frames. Then, design parameters presented in the following sections were assessed by using a specific target global inelastic deformation capacity. In this case, the maximum deformation capacity allowed in NTCS-04 (NTCS-04, 2004) for ductile systems given by $Q = 4$ was considered. Therefore, key design parameters for those models where $\mu_{global} > Q$ were computed again for a fixed global ductility $\mu_{global} = Q = 4$. Note that this strategy is used in order to account for a uniform criterion to assess global design parameters related to

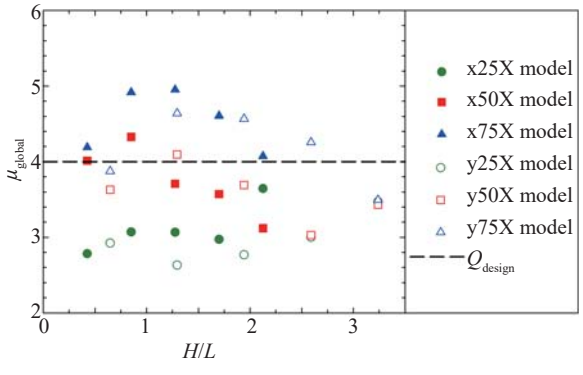

Fig. 8 Relationship of the global ductility capacity (μ_{global}) with the slenderness ratio (H/L)

a specific target global inelastic deformation capacity. As mentioned above, for seismic design purposes, the global inelastic deformation capacity, expressed through the seismic response modification factor Q in Mexican seismic guidelines, can adopt different values (Q = 1, 1.5, 2 for non-ductile systems and Q = 3, 4 for ductile systems). In this study, all the models were designed considering a uniform Q factor equal to 4 (Q = 4), so the models in which, theoretically, global inelastic deformation capacity was greater than that value, were limited precisely to the maximum value considered in the design stage.

Note that in these sections, only the results for ductile models (x50X, y50X, x75X and y75X) were included. This was done because, as mentioned above, the x25X and y25X frame models had a non-ductile behavior.

4.1 Overstrength factors (R or Ω_0)

During the past few decades, many research studies have been focused on the study of the variation of overstrength reduction factors R (Ω_0 in United States codes) and its importance on the seismic design process for different structural systems (Mitchell and Paultre, 1994; Kappos, 1999; Elnashai and Mwafy, 2002; Maheri and Akbari, 2003; Tena-Colunga *et al*., 2008; Godínez-Domínguez and Tena-Colunga, 2010; Godínez-Domínguez *et al*., 2012; Farahi and Mofid, 2013; Tapia-Hernández and Tena-Colunga, 2014; Tena-Colunga and Nangullasmú-Hernández, 2015; Tena-Colunga and Cortés-Benítez, 2015; Godínez-Domínguez and Tena-Colunga, 2016; Tena-Colunga and Hernández-Ramírez, 2017; Vona and Mastroberti, 2018). In design procedures established in current Mexican seismic codes (NTCS-04, 2004; MOC-15, 2015), an overstrength reduction factor R is used to compute the inelastic design spectra. R is obtained using Eq. (2) in NTCS-04, and it is worth noting that it was proposed using mainly the results for moment-resisting RC framed buildings (Tena-Colunga *et al.*, 2008 and 2009). In this study, the overstrength for the structural system is computed using Eq. (3).

$$R = \Omega_0 = \begin{cases} \dfrac{10}{4+\sqrt{T/T_a}} & \text{if } T \le T_a \\ 2 & \text{if } T > T_a \end{cases} \tag{2}$$

where T_a is the control period at the beginning of the plateau for the design spectrum and T is the fundamental structural period.

$$R = \Omega_0 = \frac{V_u}{V_{des}} \tag{3}$$

where V_u is the peak strength obtained from pushover curves and V_{des} is the nominal design shear force.

Overstrength reduction factors (Eq. (3)) are compared in Fig. 9(a) with those obtained by using Eq. (2). Also, in order to show the influence of the building geometry, a plot of R factors vs H/L is shown in Fig. 9(b), where H is the building height and L is the dimension in plan in the analysis direction.

From the results presented in Figs. 9(a) and 9(b), it is observed that R factors obtained for stiffer frame models are usually higher than those specified in seismic guidelines of MFDC (Eq. (2)). This is because the design of low-rise structures is usually more impacted by gravitational load combinations than for medium-rise or high-rise structures, where the design of structural members is usually governed by load combinations that consider both gravitational and seismic loads.

It is also observed that, for most ductile models, R factors are increased as the shear strength provided by the RC columns are increased. This is opposite to what was previously observed for inverted-V braced structures (Godínez-Domínguez and Tena-Colunga, 2010), where R factors decreased as the shear strength provided by the RC columns increased for models ranging from four to twelve stories.

As expected, assessed R factors using Eq. (3) are different from those computed using Eq. (2), especially for low-rise structures. However, an acceptable correlation is obtained for 12 to 20 story models. In general, proposed R values in NTCS-04 underestimate the assessed R values.

As in the design stage, where the local overstrength of the bracing system obtained in the Y direction (empty symbols) was greater than those in the X direction (filled symbols), the global R factors are usually greater precisely in the Y direction.

As observed and reported in previous studies for inverted-V braced RC structures (Godínez-Domínguez and Tena-Colunga, 2010 and 2016) and other structural systems such as inverted-V braced steel frames (Tapia-Hernández and Tena-Colunga, 2014), moment-resisting RC frames (Tena-Colunga *et al*., 2008; Tena-Colunga and Cortés-Benítez, 2015) and RC framed structures with hysteretic energy dissipation devices mounted on chevron bracing (Tena-Colunga and Nangullasmú-Hernández, 2015; Tena-Colunga and Hernández-Ramírez, 2017), R factors are highly dependent on the global geometry of the structure, expressed in this study in terms of the global slenderness relationship H/L. As shown in Fig. 9(b), it is clear that the smaller the H/L values, the greater the R factors.

4.2 Story drifts related to different limit states

Currently, in MFDC (MFDC-04, 2004), the proposed inter-story drift design value for the service limit state (Δ_{ser} = 0.004) is used for the design of any kind of building, regardless of its structural system and inherent specific lateral stiffness. In order to observe if this limit is suitable for the design of steel-X braced RC frames, a comparison between envelopes for the equivalent story drift at yielding (Δ_y) and the proposed limit are shown in Fig. 10. For all cases, the proposed limit in NTCS-04

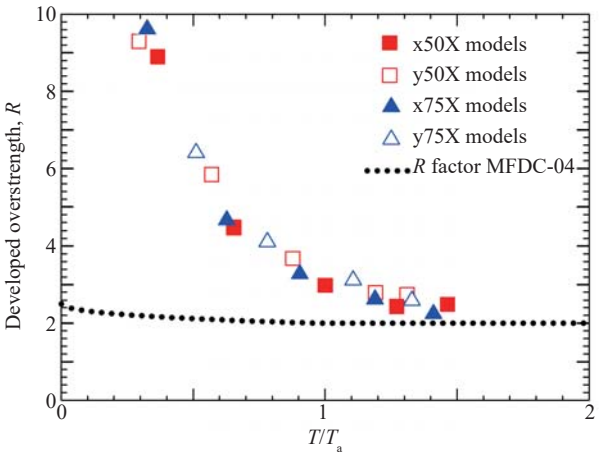

(a) Assessed R factors vs. R factors in MFDC-04

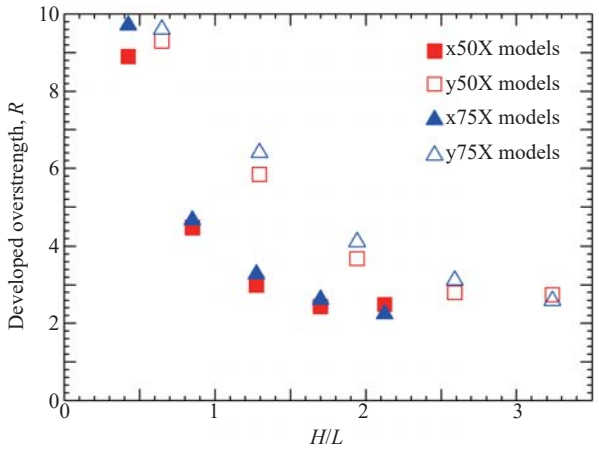

(b) Assessed R factors vs. slenderness radio (H/L)

Fig. 9 Assessed overstrength factors R (Ω_0) for a maximum global ductility capacity $\mu_{global} = 4$

(2004), indicated as the limit value on the abscissa axis, is always greater than the computed Δ_y values. Therefore, it would be desirable to assess and propose specific global design parameters for RC-MRCBFs.

Following the same criterion, envelopes for peak story drifts (Δ_{max}) were computed and are depicted in Fig. 11. These curves are helpful to evaluate peak story drift for design purposes. Opposite to what it was observed for the service limit state, from the results shown in Fig. 11, it appears that the drift limit $\Delta_{max} = 0.015$ set in modern international building codes, such as ASCE 7-10 (2010) and NTCS-04 (2004), is a good option to define the collapse prevention story drift limit (in all cases the design drift limit covers the peak drifts).

5 Nonlinear dynamic analyses

To complete the information reported in previous sections, and to assess the seismic performance of the designed models as a function of the shear strength ratios between the steel X-bracing system and the RC moment frame system, nonlinear dynamic analyses were performed by using Ruaumoko software (Carr, 2004).

From experimental and analytical studies (e.g., Black *et al.*, 1980; Ikeda *et al.*, 1984; Ikeda and Mahin, 1984; Khatib *et al.*, 1988; Remennikov and Walpole, 1997a; Dicleli and Calik, 2008; D'Aniello *et al.*, 2015), it is clear that the hysteretic behavior of bracing members is quite complex and its modelling is critical to simulate the nonlinear behavior and failure mechanism of braced systems. Two of the most used analytical models to represent the cyclic buckling behavior of steel braces for the study of dual systems usually fall into the following categories: a) phenomenological models and, b) physical-theory brace models.

As commented by Ikeda and Mahin (1984) and Uriz *et al.* (2008), phenomenological models are the simplest and most computationally efficient; in these, the brace is represented by a truss element with hysteretic behavior which reproduces the experimentally observed response (observed axial force-axial displacement curves). The limitation of this approach is the need for model calibration with available experimental data, and the limited predictive ability, since the hysteretic behavior only represents the behavior of specimens for which it was calibrated (usually, it is difficult to select the empirical input parameters without access either to appropriate experimental results or, alternatively, to the analytical results obtained using other more refined models).

On the other hand, physical-theory models

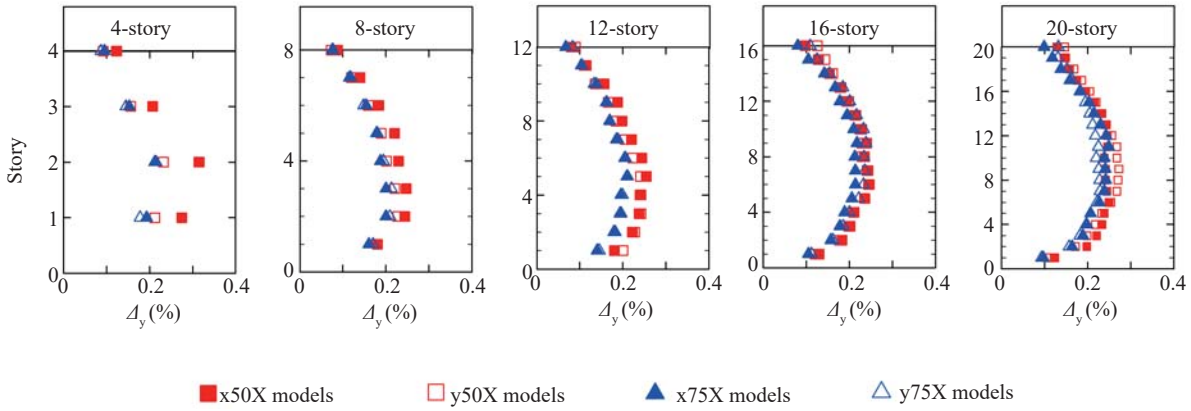

Fig. 10 Equivalent yield drift envelopes

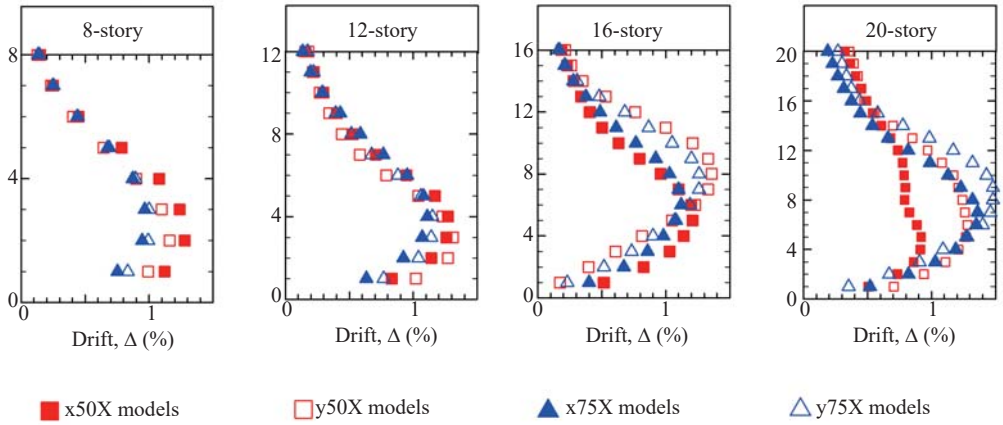

Fig. 11 Peak story drift envelopes

incorporate simplified theoretical formulations based on the physical considerations that permit the cyclic inelasticity to be computed (Ikeda and Mahin, 1984; Remennikov and Walpole, 1997a). Unlike the prior empirical information on cyclic behavior required for phenomenological models, the input parameters for physical theory models are based on the material properties and common geometric or derived engineering properties of a member (e.g., the cross sectional area, cross sectional moment of inertia, effective member length, plastic section modulus). As commented by Uriz *et al.* (2008) and D'Aniello *et al.* (2015), physical-theory models represent one of the most efficient approaches to simulate the nonlinear response of CBFs, which are test-free dependent and low time demanding in the processing of analyses. In this case, the braces are usually schematized with two elements connected by a generalized plastic hinge for the braces or accounting for distributed plasticity. An initial out-of-straightness imperfection (or camber) is introduced at the intersection of the two connected elements to reproduce the buckling of the braces. Thus, physical theory models attempt to combine the realism of finite element approaches with the computational simplicity of phenomenological modeling (Ikeda and Mahin, 1984).

In this study, the incremental physical theory brace model proposed by Remennikov and Walpole (1997a and 1997b) was used to simulate the cyclic behavior of bracing members. In this model, the analytical formulation of plastic hinge behavior is combined with empirical formulas developed on the basis of experimental data. The model proposed by Remennikov and Walpole (1997a) is largely based on the one previously proposed by Ikeda and Mahin (1984), where the experimental results developed by Black *et al*. (1980) were used to validate their proposed model.

The brace model used is able to accurately simulate the cyclic inelastic behavior of steel braces and braced systems, as demonstrated previously by Remennikov and Walpole (1995, 1997a and 1997b). This fact can be observed in Fig. 12, where a comparison of analytical and experimental results for bracing members with different boundary conditions under cyclic loading are presented. As observed from Fig. 12, in both cases, the model is suitable to simulate the shifts of yield surface during later cycles in tension, the increase in the value of the plastic moment in compression, as well as the deterioration in the buckling load with cycling. Thus, the results of the research studies developed by Remennikov and Walpole (1995, 1997a and 1997b) demonstrated that their incremental physical theory model is able to suitably represent the overall cyclic buckling behavior of bracing members. This model is currently available in the inelastic dynamic frame analysis program RUAUMOKO (Carr, 2004) to enable evaluation of the inelastic seismic response for braced structures, and it was used in this study for modeling the bracing members.

Finally, in order to capture the stiffness degradation effect of reinforced concrete members under cyclic loading, all beams and columns were modeled using the modified Takeda model proposed by Otani (Fig. 13), which is a modification of the well-known refined phenomenological Takeda model (Saiidi and Sozen, 1979). The Takeda model is based on a series of experimental results of reinforced concrete subassemblages. The modified Takeda model is problem-free, numerically stable and comprehensive, which is why it has been implemented in different computer programs (e.g., DRAIN-2D, ANSR and RUAUMOKO) and is suitable to represent the inelastic behavior of RC members. The alfa (α) and beta (β) parameters shown in Fig. 13 are used to control the unloading and reloading stiffness. Thus, increasing α decreases the unloading stiffness and increasing β increases the reloading stiffness.

5.1 Earthquake input excitations

To be consistent with the seismic hazard specified in NTCS-04, artificial records were obtained for the studied zone. Artificial records were obtained using a method where the records of small ($M_s < 6$) or moderate

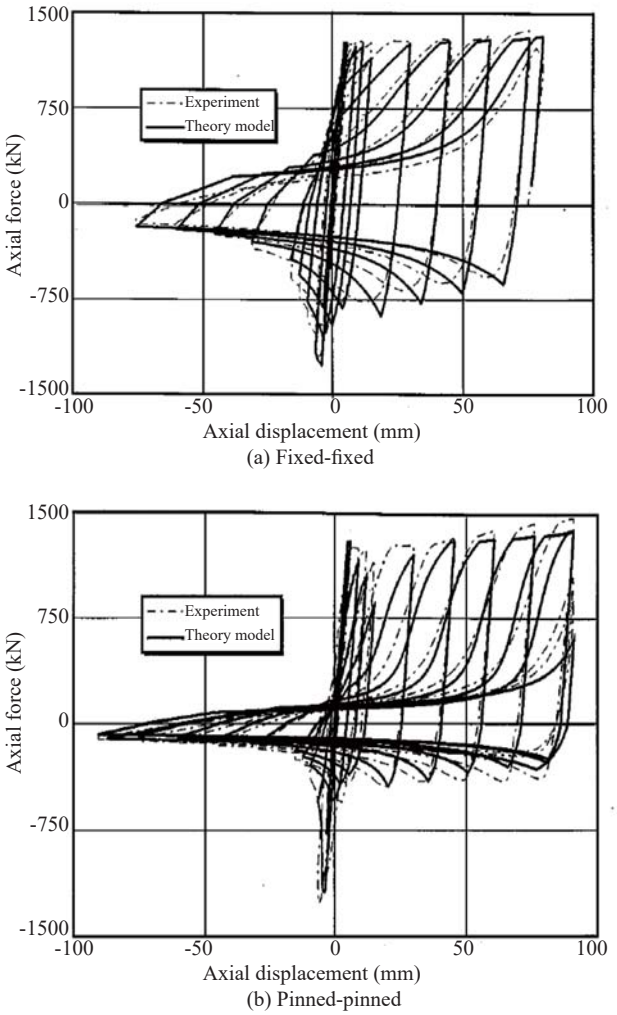

Fig. 12 Comparison of analytical and experimental *P-δ* curves for fixed-fixed and pinned-pinned brace members (Remennikov and Walpole, 1997a)

($6 < M_s < 7$) earthquakes are used to simulate the motions produced by greater earthquakes (Hartzell, 1978). This method is based on the hypothesis that the complexity observed in the recorded ground motions will be present in earthquakes of greater magnitude that would occur in the same epicentral region. The effects attributed to the seismic source (discontinuities in the area of contact between plates, directivity effects, speed of rupture, particularities of the energy irradiation, etc.) and the distance from the source or trajectory (mainly attenuation) is preserved in small and strong earthquakes (Pérez-Rocha, 1998).

The procedure used for obtaining synthetic acceleration records considers the use of the updated average empirical transfer functions (ETF) at the site of interest (soft soils) and the average fourier amplitude spectra (FAS) corresponding to firm soils. For this study, the average FAS obtained for the outcrop CU01 station in Mexico City is taken as the average FAS for firm soils in Mexico City, in absence of recording stations at the base of the soft-soil deposits within Mexico City's Metropolitan Area. During the scaling process of the seismic source, the recorded ground motions for the selected stations for the April 25, 1989 earthquake (M = 6.9) were used as Green's functions (Hartzell, 1978; Pérez-Rocha, 1998).

The methodology used for the generation of the artificial records, briefly outlined above, is discussed in detail elsewhere (Pérez-Rocha, 1998; Tena-Colunga *et al*., 2007; Godínez-Domínguez *et al.*, 2012). Nine artificial records and their corresponding pseudo acceleration spectra for 5% equivalent viscous damping used for the dynamic analyses are depicted in Fig. 14. Design spectra are also depicted in Fig. 14.

5.2 Processed information

As a first step, story and global hysteresis curves were obtained from nonlinear dynamic analyses. Then, using that information, some envelopes proposed by Tena-Colunga *et al.* (2008) were computed, as illustrated in Fig. 15. As was done in pushover analyses, Δ_y was defined according to what was proposed by Newmark and Hall (1982).

As discussed by Tena-Colunga *et al.* (2008), "half cycles were considered for assessing k_{ave} because of the important differences often observed in the amplitude of adjacent positive and negative half cycles due to the variation of the intensity of the ground motion". Some of the concepts mentioned above that are discussed in these sections are schematically presented in Fig. 15. Peak and average responses for all the envelopes are presented and discussed in following section.

Finally, the authors present an evaluation of the achieved collapse mechanisms and also a brief discussion of the residual drifts, residual drift ratios, mappings of residual deformations in steel braces and residual rotations in RC beams and columns (peak and average responses).

For space constrains, only representative results for models ranging from 12 to 20 stories in the X-direction

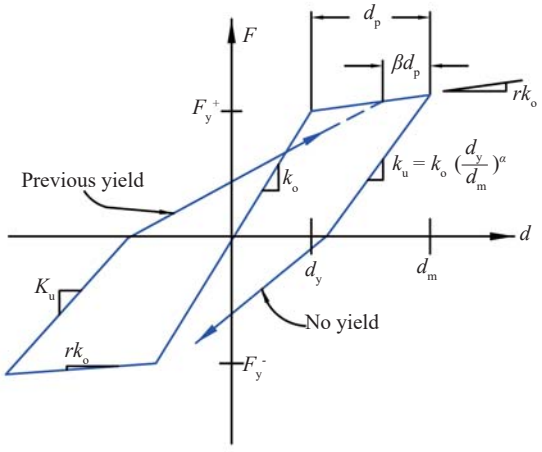

Fig. 13 Modified Takeda hysteresis model used for modeling of RC members (adapted from Carr, 2004)

are presented and discussed in this section.

The hysteresis curves shown in Figs. 16-18 correspond to the 12, 16 and 20 story models, respectively, considering the acceleration record that generated response maxima.

It can be observed from the hysteresis curves that, in some cases, when the bracing system represents the main line of defense of the structural system (non-ductile models, e.g., Fig. 16(a)), an unstable response could be obtained. In fact, for 20-story models, an unstable response was obtained for all the analyses, so in this section, for an efficient use of space, only results for 20-story ductile models are reported (20x50X and 20x75X models). Nevertheless, as the contribution of the RC columns to the global strength and stiffness increases, an improvement in the structural behavior is observed, getting a better energy dissipation capacity and a more stable cyclic behavior (Figs. 16(b)-(c), 17(b)-(c)). This effect is very simple to observe for 12-story models. The above observation is in good agreement with the pushover analyses results.

Envelopes of average response maxima (average of peak responses for the nine studied records) and response maxima (peak responses for the most critical record) were obtained from the hysteretic curves and the corresponding results are shown in Figs. 19 to 21 for

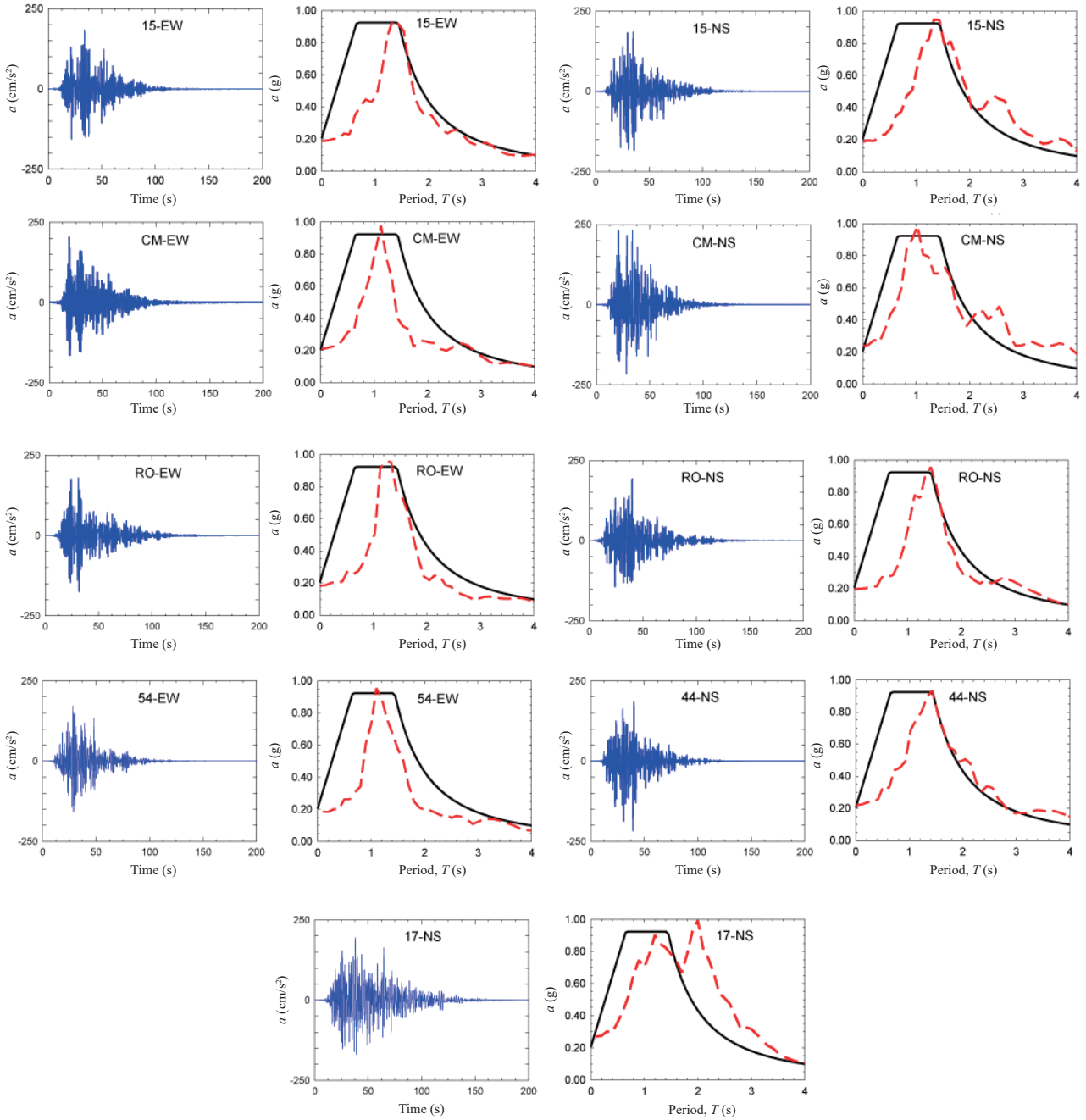

Fig. 14 Artificial acceleration records for the lake bed zone of Mexico City

the 12, 16 and 20-story models. As can be seen from Figs. 19(a1), 19(b1), 20(a1), 20(b1), 21(a1) and 21(b1), for all building heights and shear strength ratios, story drifts at first yield (Δ_{fe}) increases slightly as the number of stories increases. Similar tendencies are observed for all models when comparing Δ_{fe} envelopes (maxima and average maxima) to the corresponding envelopes for the equivalent story drift at yielding (Δ_y, Figs. 19(a2), 19(b2), 20(a2), 20(b2), 21(a2) and 21(b2)). However, higher values are always obtained in the last case. Envelopes for ductile models have similar values in all cases. For each building height, the greater Δ_y values usually correspond to non-ductile models, where the steel bracing represents the main line of defense of the structural system (models 12x25X, 16x25X and 20x25X). As expected, and in agreement with the results previously obtained in pushover analyses, Δ_y envelopes for ductile models are always smaller than the corresponding story drift limit for the "service" earthquake defined in NTCS-04 (Δ_{ser} = 0.004). However, for non-ductile models, the currently proposed design limit could be a good alternative for the story drift limit for the service earthquake.

From envelopes of dynamic story drift angles (Figs. 19(a3), 19(b3), 20(a3), 20(b3), 21(a3) and 21(b3)), it is possible to conclude again that the limit currently proposed in ASCE 7-10 (2010) and NTCS-04 (2004), is a good choice for the collapse prevention story drift limit; even though some peak demands (maxima, i.e., 12x75X and 16x50X) exceed that limit. Note that the limit proposed by these international building codes (Δ_{max} = 0.015) always cover the average response envelopes.

Curves for the equivalent number of nonlinear cycles are presented in Figs. 19(a4), 19(b4), 20(a4), 20(b4), 21(a4) and 21(b4). Also, curves for k_{ave}/k_{el} are shown in Figs. 19(a5), 19(b5), 20(a5), 20(b5), 21(a5) and 21(b5) for the 12, 16 and 20 story models, respectively. Finally, envelopes for peak dynamic story ductility demands (μ) are plotted in Figs. 19(a6), 19(b6), 20(a6), 20(b6), 21(a6) and 21(b6).

From the response maxima envelopes, it is appreciated that all twelve-story models experienced a similar number of inelastic cycles. Nevertheless, greater reductions of the stiffness are obtained in the non-ductile model (12x25X) and correspond to an unstable cyclic behavior (Fig. 16(a)). For ductile 12-story models (12x50X and 12x75X), smaller ductility demands are observed compared to the non-ductile model. From average response envelopes, it is observed that a greater inelastic behavior is demanded in ductile models. However, in spite of that, a more stable cyclic behavior is always observed in ductile models than in non-ductile models.

It can be observed from average response curves for 16 and 20-story models that the highest number of inelastic cycles occurs from the 2nd to the 12th story, which is consistent with the observed hight-wise stiffness degradation. Note that for the 16 story non-ductile models, although the ductility demands are usually smaller than those obtained for ductile models, the stiffness degradation is very similar to that obtained for ductile models (where greater ductility demands are observed), especially when average response envelopes are considered (Figs. 20(b5)-(b6)). This is because, although the ductility demands are usually small, the number of inelastic cycles is high and these cycles have large amplitudes (Figs. 17(a), 20(a4) and 20(b4)). For the 20-story ductile models, very similar results were obtained for both response maxima and average response maxima (Fig. 21).

5.3 Mapping of accumulated plastic rotations

As previously done for pushover analyses, and following the same objective, yielding mappings were obtained for all the models (Fig. 22). The same marks and color scales were used as in the previous mappings.

As observed in pushover analyses (Fig. 7), it was found that for non-ductile models (Figs. 22(a)-(c)), the failure mechanism is not ductile, and braces are not the first line of defense under lateral loading. Actually, the first plastic hinges always occur in beams.

The sequence of the formation of the failure

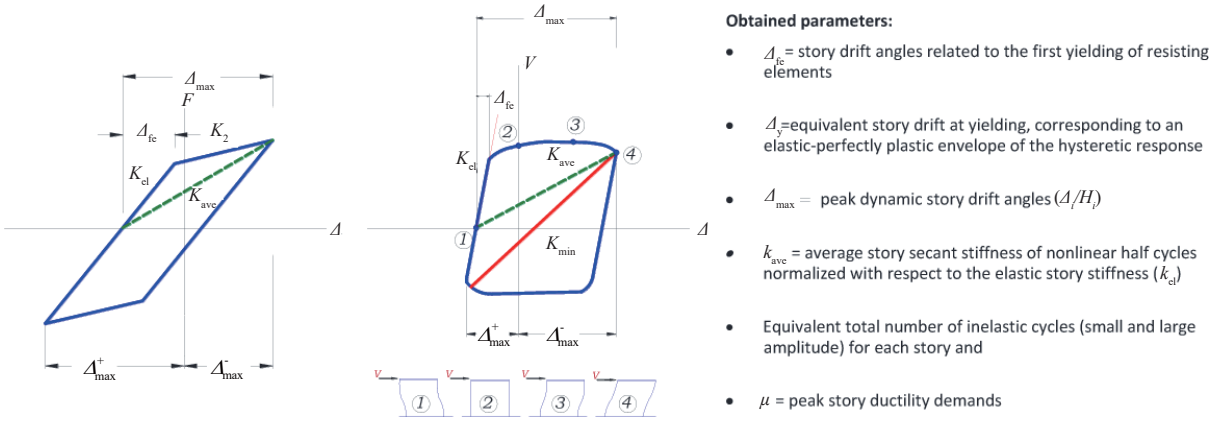

Fig. 15 Schematic representation of the studied dynamic parameters (Tena-Colunga *et al.*, 2008)

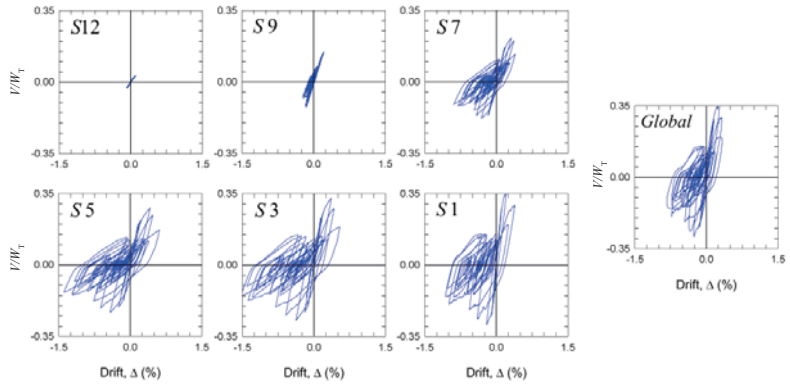

(a) 12x25X

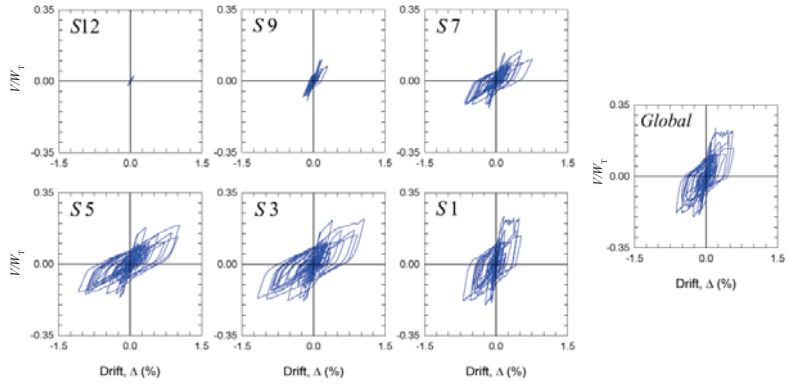

(b) 12x50X

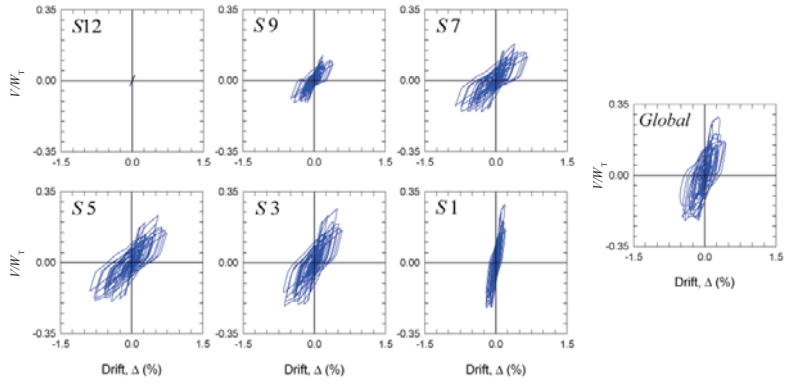

(c) 12x75X

Fig. 16 Normalized story and global hysteresis curves (V/W_T vs Δ) for twelve-story models under the action of the CM-NS acceleration record that generate the response maxima

mechanisms (i.e., the development of the first plastic hinge in beams or the first plastic deformation in braces) is also dependent on the height of the studied building, as was previously observed for RC inverted V braced frames (Godínez-Domínguez and Tena-Colunga, 2010 and 2016; Godínez-Domínguez *et al.*, 2012) and for RC diagonal braced frames (Eskandari *et al.*, 2017).

For ductile frame models (Figs. 22(b)-(c), 22(e)-(f), 22(g)-(h)), similar yielding mappings are observed in spite of the different shear strength balance considered in each case. The collapse mechanisms obtained for ductile models ranging from four to sixteen stories compare reasonably well with the anticipated one. These results are in good agreement with pushover analyses results and also with the findings of other studies where different steel bracing configurations were used (Godínez-Domínguez and Tena-Colunga, 2010 and 2016; Godínez-Domínguez *et al.*, 2012; Eskandari *et al.*, 2017). From pushover analyses, it was observed that for the taller models (20-stories), some plastic rotations are formed at the column ends in the bottom stories. Nevertheless, such an effect is not observed in the results obtained from nonlinear dynamic analyses, especially for ductile models, where good structural behavior is achieved. Therefore, from these and previous results, it can be concluded that an additional increment in the shear strength contribution

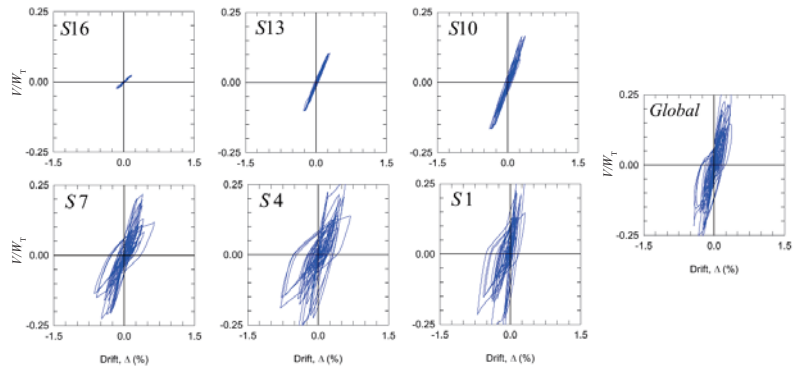

(a) 16x25X

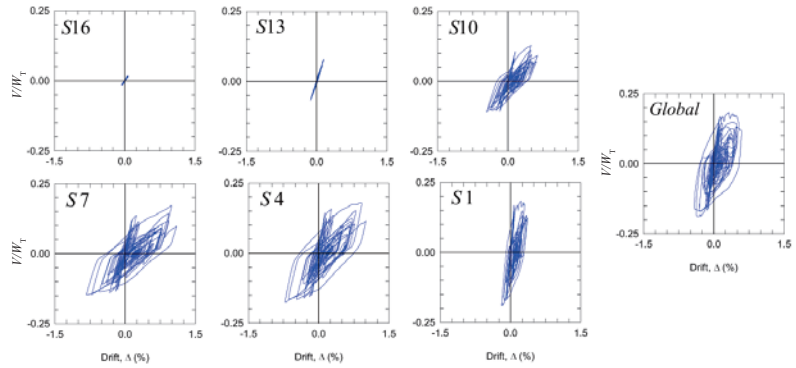

(b) 16x50X

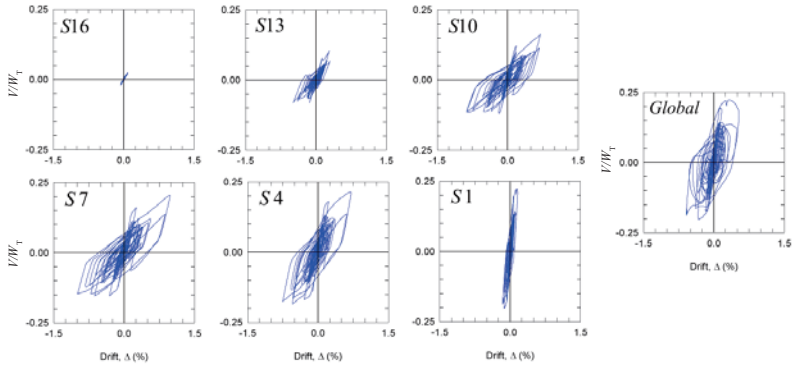

(c) 16x75X

Fig. 17 Normalized story and global hysteresis curves (V/W_T vs Δ) for sixteen-story models under the action of the 17-NS acceleration record that generated the response maxima

design requirement for the RC columns to endure lateral seismic loads, as the building height increases, could represent an adequate strategy to improve the seismic behavior of this dual system.

5.4 Residual drifts

This section is focused on evaluating the amplitude and height-wise distribution of residual drifts after earthquake excitation as a function of the considered shear strength balance. Among others, residual drift of a structure depends on the hysteretic behavior, earthquake ground motion, frame mechanism and overstrength (Ruiz and Miranda, 2006; Henry *et al.*, 2016).

As described by Henry *et al.* (2016), "a residual displacement observed from a cyclic hysteresis loop does not necessarily warrant poor building performance. This is because the residual drift of a structure subjected to an earthquake depends on the peak drift that the structure experiences, as well as its dynamic response during the remainder of the earthquake duration and the free vibration that occurs at the end of an earthquake input motion". This post-peak behavior, referred to by McRae and Kawashima in 1997 as the "shake-down" phenomenon, is illustrated in Fig. 23 (Henry *et al.*, 2016). Then, the residual drift at the end of the dynamic response (d_r) will normally be smaller than the peak residual drift instantaneously following the peak lateral

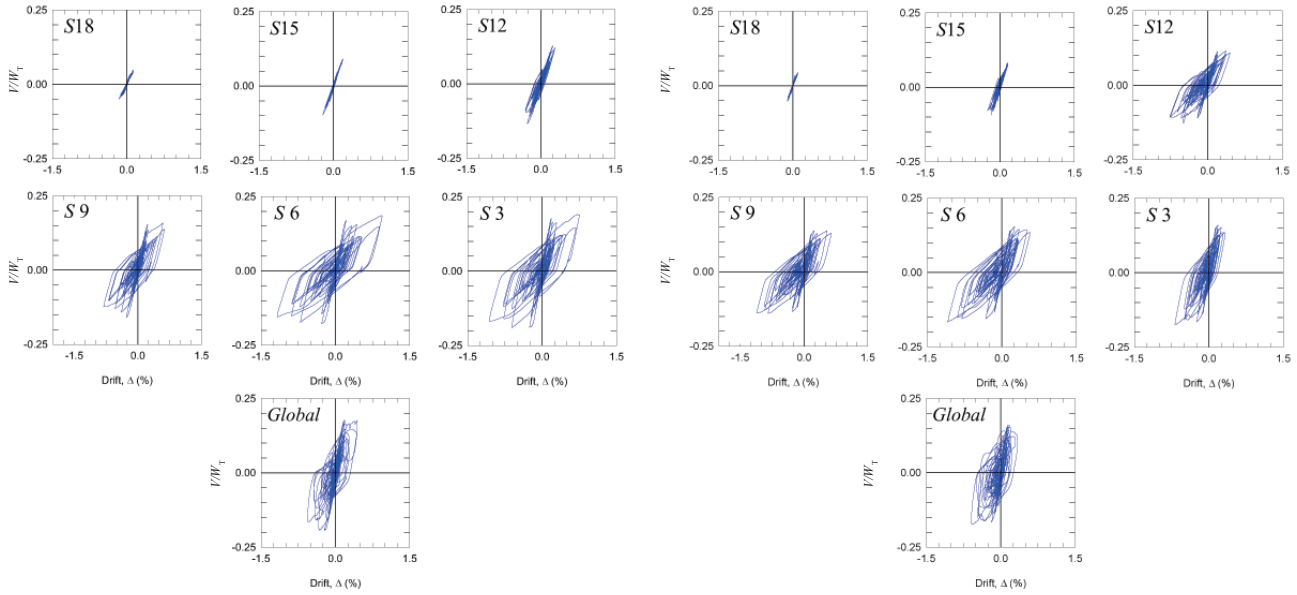

(a) 20x50X (b) 20x75X

Fig. 18 Normalized story and global hysteresis curves (V/W_T vs Δ) for 20-story models under the action of the CM-NS acceleration record that generated response maxima

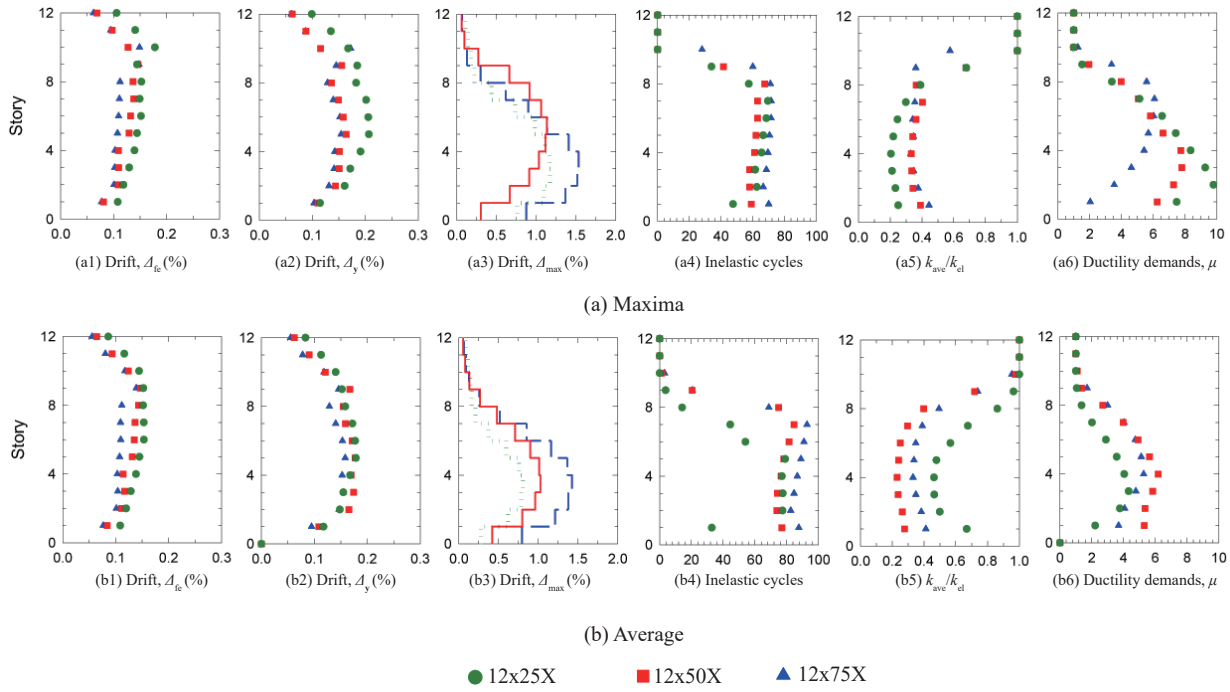

Fig. 19 Envelopes of response maxima and average response maxima for 12-story models

drift (d_{rmax}).

In order to quantify the effectiveness of the shake-down effect, in addition to the residual drifts, a residual drift ratio proposed by MacRae and Kawashima in 1997 (Henry *et al.*, 2016) was computed in this section. As reported by Henry *et al.* (2016), the residual drift ratio, d_{rr}, was calculated by dividing the residual drift at the end of the analysis, d_r, by the maximum possible residual drift, d_{rmax}, which is the residual drift when unloading immediately after the maximum lateral displacement (also referred to as maximum static or cyclic residual drift). Finally, an extra non-dimensional parameter was computed, dividing the residual drift at the end of the analysis, d_r, by the maximum drift, d_{max}. Residual drift (d_r) and normalized residual drifts (d_r/d_{rmax} and d_r/d_{max}) are plotted in Fig. 24 for 12, 16 and 20 story models.

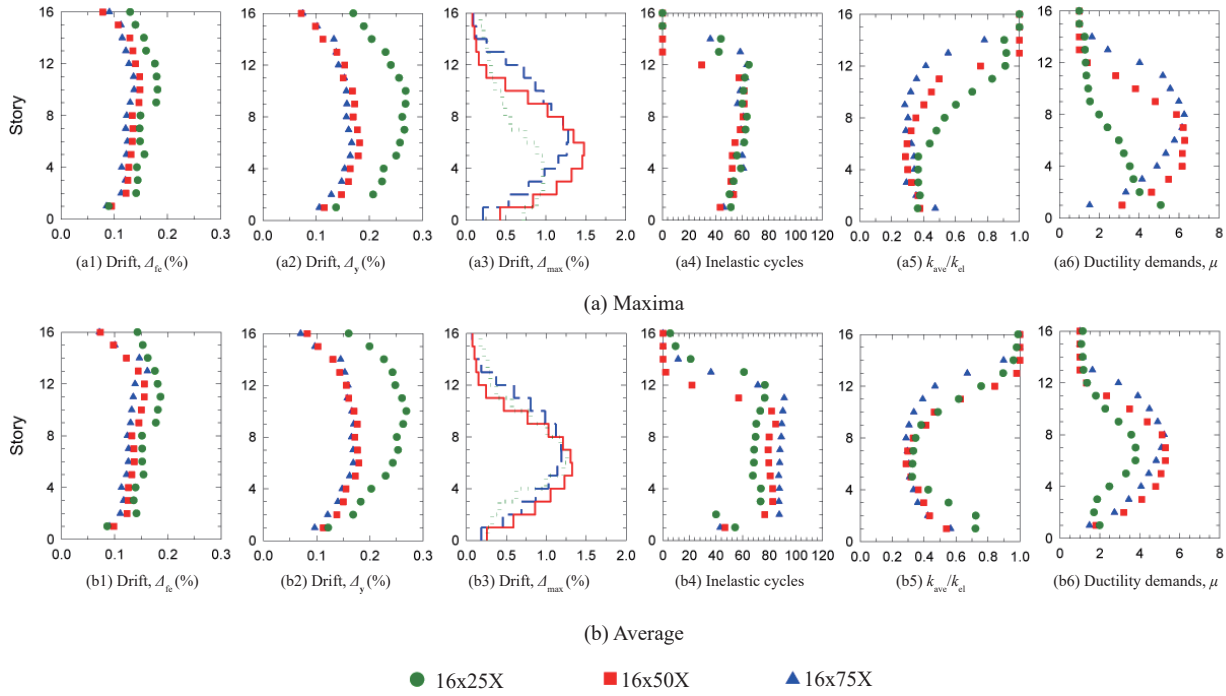

Fig. 20 Envelopes of response maxima and average response maxima for 16-story models

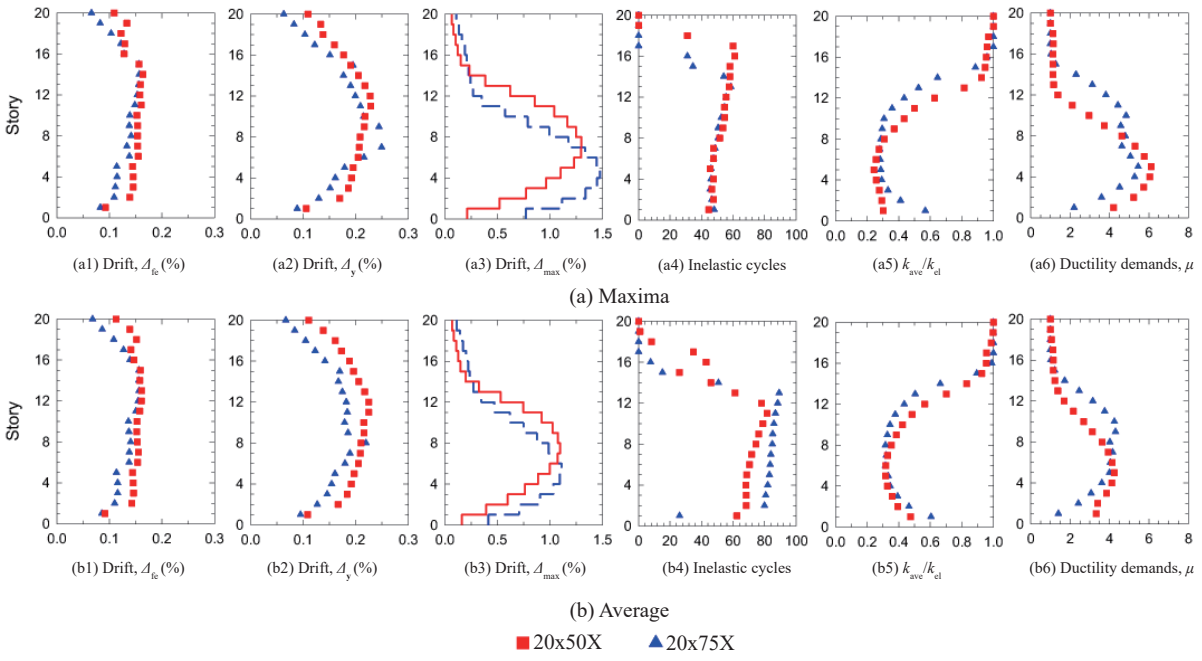

Fig. 21 Envelopes of response maxima and average response maxima for 20-story models

For 12-story models, when considering maximum responses, the computed residual drifts (d_r) and residual drift ratios (d_r/d_{rmax} and and d_r/d_{max}) for non-ductile models (x25X models) are greater than those obtained for ductile models (x50X and x75X models). However, for average responses, d_r, d_r/d_{rmax} and d_r/d_{max} values for ductile models are in general greater than those obtained for non-ductile models. Residual drifts (d_r curves) obtained for ductile models are almost identical.

As expected, for ductile models, peak residual drifts for the critical record obtained for 12 story models are smaller than those obtained for 16 and 20 story models. It is also observed from average peak responses that for most models (i.e., 12x25X, 12x50X, 12x75X, 16x25X, 20x50X), the shape of the residual drift envelopes are similar to the peak dynamic story drift envelopes. This observation was also found by Ruiz and Miranda (2006) for regular multi-story moment frames. In fact, this

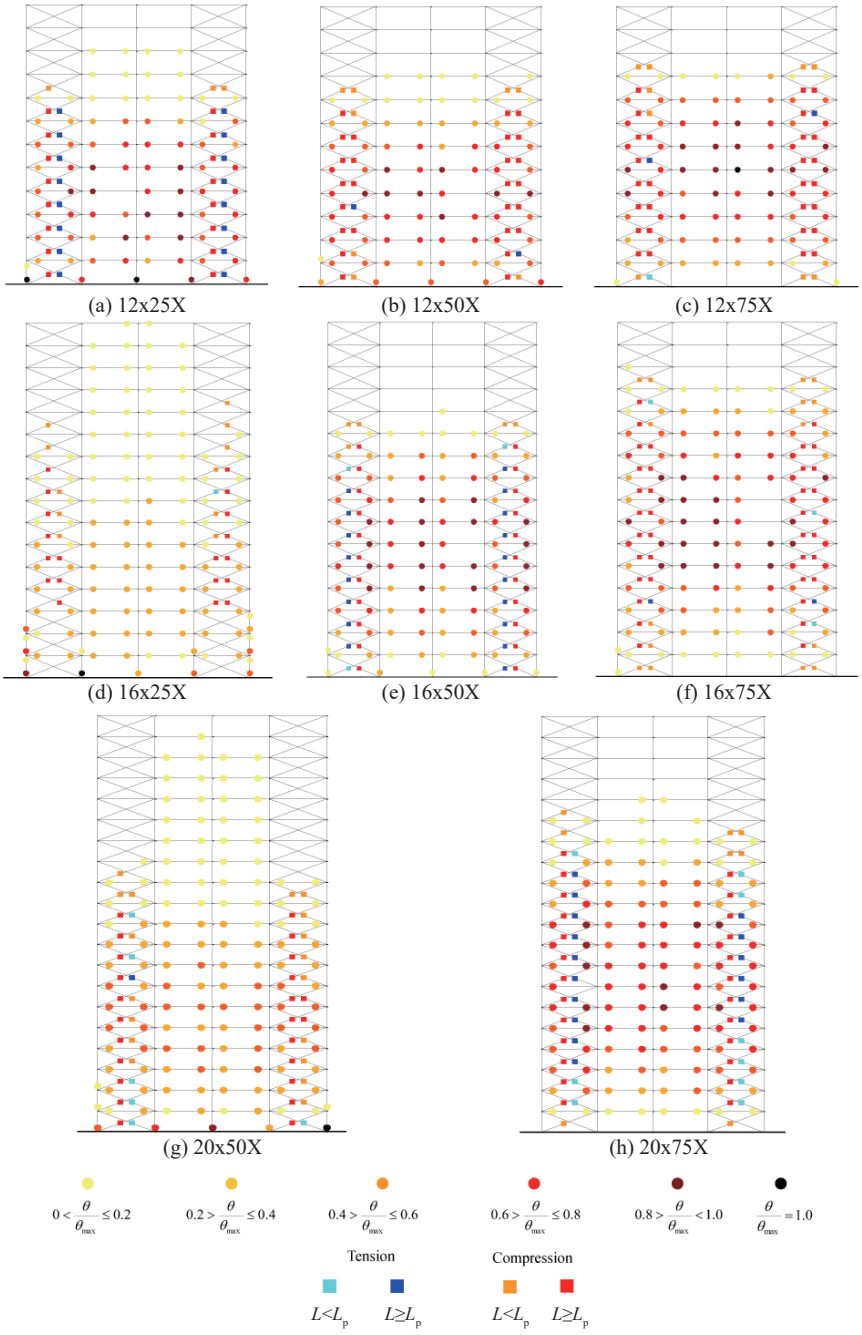

Fig. 22 Mapping of accumulated plastic rotations for 12, 16 and 20 story models in the *X* direction under the action of the acceleration record that generated the response maxima

observation is also supported in several reconnaissance reports of severely damaged buildings after the occurrence of strong earthquakes.

The highest average story residual drift ratios ($d_r = d_r/d_{rmax}$) for 12, 16 and 20 story ductile models were computed to be 0.52, 0.46 and 0.36 (Fig. 24), the meaning of which is that the shake-down effect lessens the residual drift, on average, to less than 52%, 46% and 36% of the maximum possible residual drifts, respectively. If the second normalized parameter d_r/d_{max} is considered, the above values decrease to 0.23, 0.15 and 0.17 for 12, 16 and 20 story ductile models, respectively (Fig. 24). There is no clear trend regarding the effect of the shear strength ratio on residual drift ratios, d_{rr}. However, if only ductile models are considered, it is possible to observe that the height-wise distribution of residual drifts decrease as the shear strength contribution of the columns to withstand lateral seismic forces increases.

It is important to note that current seismic provisions do not provide a specific limit value on residual drifts related to the global performance level for RC-XBFs. However, according to FEMA-356 (2000), for concrete frames, residual drifts should not exceed 1% for Life Safety and 4% for Collapse Prevention performance

levels, and for Braced Steel Frames, these limits are 0.5% and 2%, respectively.

As a complement to the information shown in Fig. 24, mappings of residual deformations and residual rotations in structural elements are plotted in Fig. 25 for the acceleration record that generates the response maxima. As can be observed from Fig. 25, the location and magnitude of residual deformations in braces and rotations in beams are directly related, in addition to the shape of the residual drifts envelopes, to the peak dynamic story drift envelopes and the corresponding mappings of accumulated plastic rotations shown in Fig. 22.

It is also observed that for ductile models, as the shear strength contribution of the RC columns increases, the distribution and magnitude of residual rotations in beams decreases, which is more evident for 20-story models (Figs. 25(g)-(h)). This is consistent with the results obtained from average residual drifts envelopes shown in Figs. 24(b1), 24(d1) and 24(f1). Therefore, from the analysis of these results, it can be concluded again that in order to get a better structural behavior, an improved strategy for the design of RC braced buildings could be to consider an increment on the shear strength contribution of RC columns to resist seismic forces as a function of the building height.

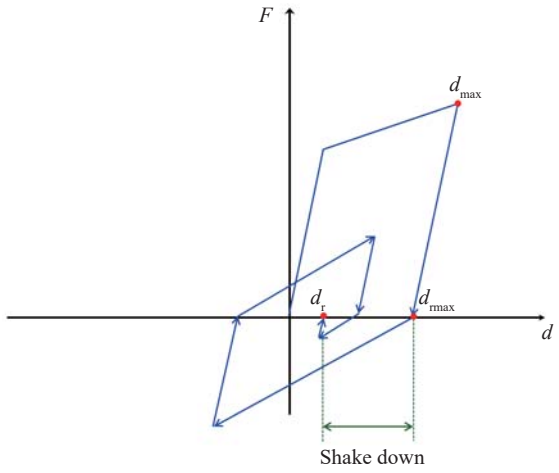

Fig. 23 Dynamic shake-down behavior (adapted from Henry *et al*., 2016)

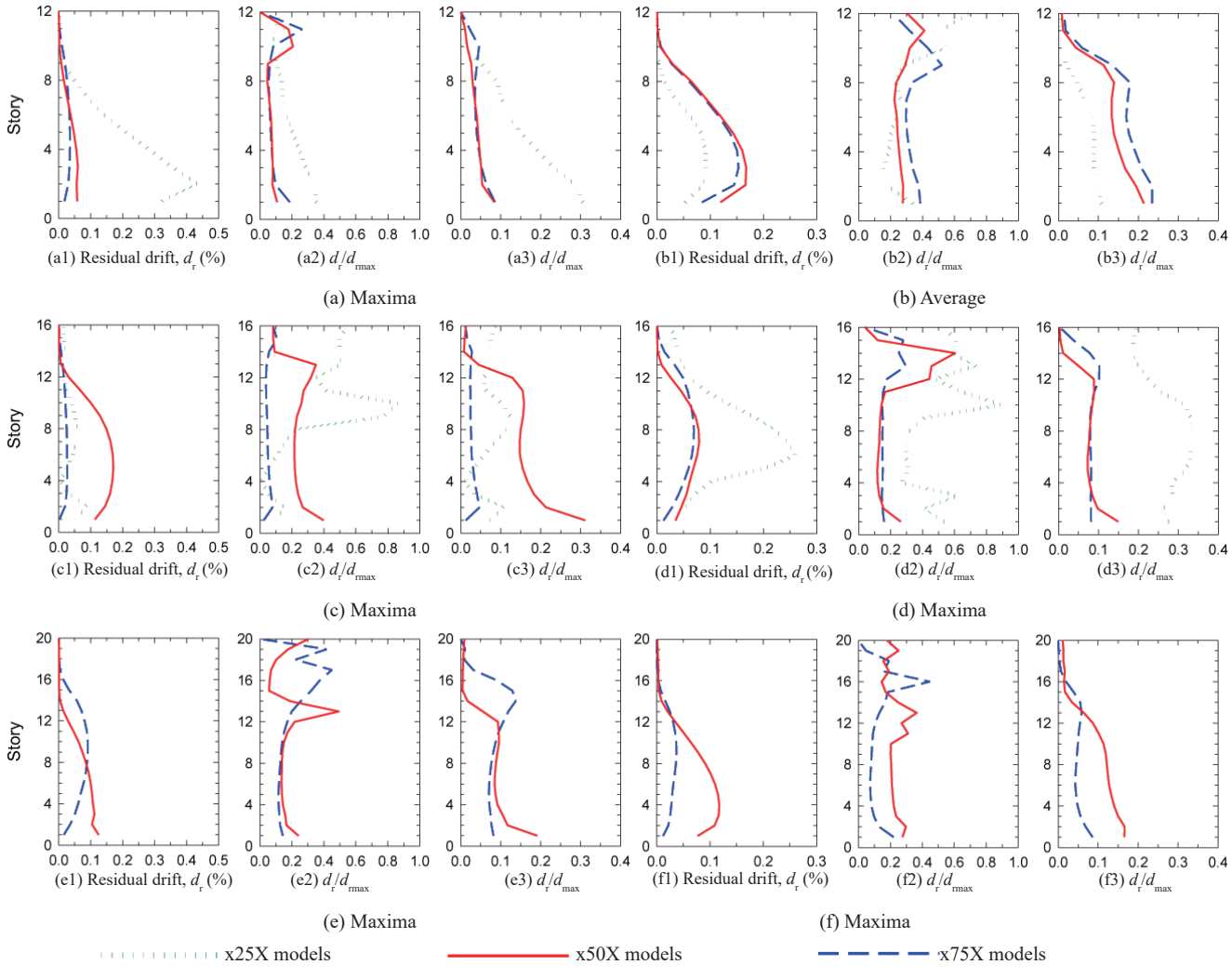

Fig. 24 Absolute and normalized residual drifts for 12, 16 and 20-story models

6 Concluding remarks

The nonlinear behavior of low to medium rise ductile RC-MRCBFs using steel X-bracing prone to buckling was assessed in this study. The height of the structures ranged from 4 to 20 stories and they were located in the lake-bed zone in Mexico City for design purposes. The structural design was carried out considering the variable contribution of the two main lines of defense of the dual system (RC columns and steel-X braces).

From the results shown and discussed herein, the following conclusions are drawn:

(1) For most models, a relationship between the assessed overstrength factors (R) and the shear strength balance between the two main components of the dual system is observed. Assessed R factors increase as the shear strength contribution of the RC columns increases. In general, proposed R values in NTCS-04 underestimate the assessed R values. Thus, an adjustment to the current NTCS-04 equation seems to be necessary in order to obtain values consistent with the analytical results, especially for the stiffer models.

(2) From the comparison of results with previous studies, it was observed that R factors depend on the bracing scheme and layout. Thus, it may be necessary to define different equations to assess R values as a function

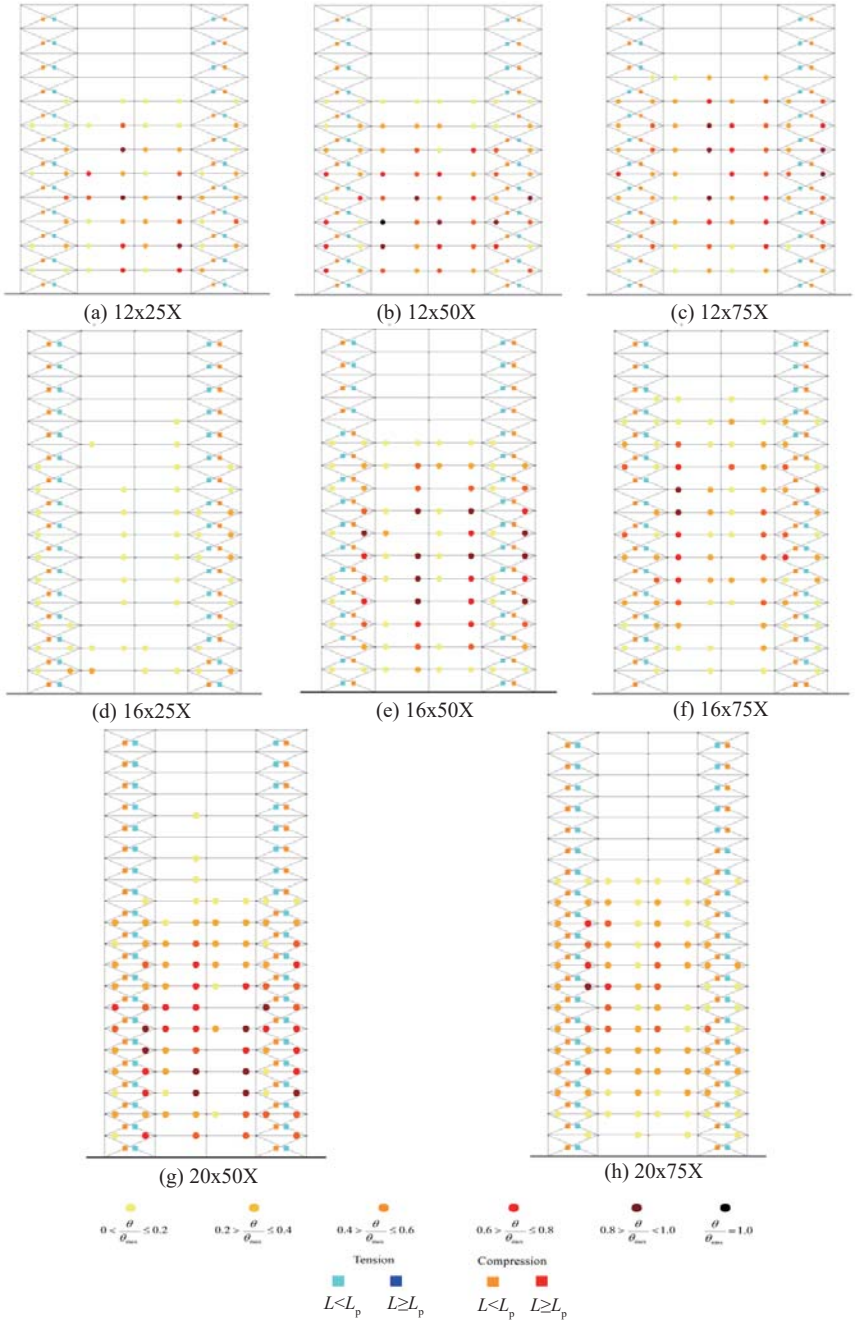

Fig. 25 Mapping of residual deformations and rotations corresponding to the acceleration record that generated the response maxima

of the bracing configuration.

(3) From the computed story yield drift envelopes, it was observed that the corresponding story drift limit for the service earthquake specified in NTCS-04 ($\Delta_{ser} = 0.004$) should be modified and reduced in order to take into account the specific stiffness of the dual system under consideration.

(4) Opposite to what was observed for the service limit state, it was observed that the inter-story drift limit $\Delta_{max} = 0.015$ established in modern international building codes, such as ASCE 7-10 (2010) and NTCS-04 (2004), is a good proposal for the collapse prevention story drift limit, since in all cases the design drift limit covers the peak static and dynamic story drift envelopes, especially when average responses are considered.

(5) It was observed from the hysteresis curves that, in some cases, when the bracing system represents the strongest or main line of defense of the structural system, an unstable dynamic response could be obtained. Nevertheless, as the contribution of the RC columns to the global strength and stiffness increases, an improvement in the structural behavior is observed, achieving a better energy dissipation capacity and a more stable cyclic behavior. Therefore, from the results of nonlinear static and dynamic analyses, it is possible to conclude that, if both a suitable design methodology and adequate shear strength ratios are taken into account, good structural behavior of new RC-MRCBFs with steel-X bracing could be achieved.

(6) Shake-down was an important effect for reducing residual drifts to less than 52%, 46% and 36% of their possible maxima for 12, 16 and 20 story models, respectively. There was no clear trend regarding the effect of the shear strength ratio on residual drift ratios, d_{rr}. However, if only ductile models are considered, it is possible to observe that the height-wise distribution of residual drifts decreases as the shear strength contribution of the columns to resist lateral seismic forces increases. Currently, specific limiting values on residual drift related to the global performance level for RC-MRCBFs are not provided in seismic design guidelines of official building codes.

(7) The location and magnitude of residual deformations in braces and rotations in beams and columns are directly related, in addition to the shape of the residual drifts envelopes, to the peak dynamic story drift envelopes and the corresponding mappings of accumulated plastic rotations.

(8) For ductile models, as the shear strength contribution of the RC columns increases, the distribution and magnitude of residual rotations in beams decreases, which is consistent with results obtained from average residual drifts envelopes. Therefore, it can be concluded again that in order to obtain a better structural behavior, an improved strategy for the design of RC braced buildings could be to consider an increment of the shear strength contribution of the frame to endure seismic forces as a function of the building height.

Acknowledgment

The support granted to the first author by the National Science and Technology Council of Mexico (Conacyt) is gratefully acknowledged.

References

Abou-Elfath H and Ghobarah A (2000), "Behaviour of Reinforced Concrete Frames Rehabilitated with Concentric Steel Bracing," *Canadian Journal of Civil Engineering*, **27**(3): 433–444.

Almeida A, Ferreira R, Proença JM and Gago AS (2017), "Seismic Retrofit of RC Building Structures with Buckling Restrained Braces," *Engineering Structures*, **130**(1): 14–22.

Aschheim M, Gülkan P, Sezen H, Bruneau M, Elnashai A, Halling M, Love J and Rahnama M (2000), "Kocaeli, Turkey, Earthquake of August 17, 1999: Reconnaissance report, Chapter 11 - Performance of Buildings," *Earthquake Spectra*, **16**(Supplement A): 237–279.

ASCE 7-10 (2010), *Minimum Design Loads for Buildings and Other Structures*, ASCE Standard ASCE/SEI 7-10, American Society of Civil Engineers, ISBN 978-0-7844-1085-1.

Aval BSB, Kouhestani HS and Mottaghi L (2017), "Effectiveness of Two Conventional Methods for Seismic Retrofit of Steel and RC Moment Resisting Frames Based on Damage Control Criteria," *Earthquake Engineering and Engineering Vibration*, **16**(3): 537–555. https://doi.org/10.1007/s11803-017-0404-y.

Badoux M and Jirsa J (1990), "Steel Bracing of RC Frames for Seismic Retrofitting," *ASCE Journal of Structural Engineering*, **116**(1): 55–74.

Barbagallo F, Bosco M, Marino EM, Rossi PP and Stramondo PR (2017), "A Multi-Performance Design Method for Seismic Upgrading of Existing RC Frames by BRBs," *Earthquake Engineering and Structural Dynamics*, **46**(7):1099–1119.

Black R, Wenger W and Popov E (1980), "Inelastic Buckling of Steel Struts under Cyclic Load Reversals," *Report No. UCB/EERC-80/40*, Department of Civil Engineering, University of California at Berkeley.

Borja-Navarrete G, Díaz-Canales M, Vázquez-Vera A and Del Valle-Calderón E (1986), "Damage Statistics of the September 19, 1985 Earthquake in Mexico City," *Proceedings of International Workshop The Mexico City Earthquakes-1985,* Factors Involved and Lessons Learned, ASCE, 70–77.

Bush T, Jones E and Jirsa J (1991), "Behavior of RC Frame Strengthened using Structural Steel Bracing," *ASCE Journal of Structural Engineering*, **117**(4): 1115–1126.

Carr AJ (2004), *RUAUMOKO: Computer Program Library*, Department of Civil Engineering, University of

Canterbury, New Zealand.

Del Valle E (1980), "Some Lessons from the March 14, 1979 Earthquake in Mexico City," *Proceedings of 7th World Conference on Earthquake Engineering*, Istanbul, Turkey, **4** (Part 1): 545–552.

D'Aniello M, La Manna Ambrosino G, Portioli F and Landolfo R (2015), "The Influence of Out-of-Straightness Imperfection in Physical Theory Models of Bracing Members on Seismic Performance Assessment of Concentric Braced Structures," *The Structural Design of Tall and Special Buildings*, **24**(3): 176–197.

Del Valle E, Foutch DA, Hjelmstad KD, Figueroa-Gutiérrez E and Tena-Colunga A (1988), "Seismic Retrofit of a RC Building: a Case Study," *Proceedings, 9th World Conference on Earthquake Engineering*, Tokyo-Kyoto, Japan, VII: 451–456.

Della Corte G, D'Aniello M and Landolfo R (2015), "Field Testing of All-Steel Buckling Restrained Braces Applied to a Damaged Reinforced Concrete Building," *Journal of Structural Engineering*, **141**(1): D4014004.

Dicleli M and Calik EE (2008), "Physical Theory Hysteretic Model for Steel Braces," *Journal of Structural Engineering-ASCE*, **134**(7): 1215–1228.

Downs RE, Hjelmstad KD and Foutch DA (1991), "Evaluation of Two RC Buildings Retrofit with Steel Bracing," *Structural Research Series No. 563*, Department of Civil Engineering, University of Illinois at Urbana-Champaign.

Elnashai AS and Mwafy AM (2002), "Overstrength and Force Reduction Factors of Multistorey Reinforced-Concrete Buildings," *The Structural Design of Tall Buildings*, **11**(5): 329–351.

El-Sokkary H and Galal K (2009), "Analytical Investigation of the Seismic Performance of RC Frames Rehabilitated Using Different Rehabilitation Techniques," *Engineering Structures*, **31**(9): 1955–1966.

Eskandari R, Vafaei D, Vafaei J and Shemshadian ME (2017), "Nonlinear Static and Dynamic Behavior of Reinforced Concrete Steel-Braced Frames," *Earthquakes and Structures*, **12**(2): 191–200.

Faella C, Lima C, Martinelli E and Realfonzo R (2014), "Steel Bracing Configurations for Seismic Retrofitting of a Reinforced Concrete Frame," *Proceedings of the Institution of Civil Engineers - Structures and Buildings*, **167**(1): 54–65.

Foutch DA, Hjelmstad KD, Del Valle E, Figueroa E and Downs RE (1989), "The Mexico Earthquake of September 19, 1985. Case Studies of Seismic Strengthening for Two Buildings in Mexico City," *Earthquake Spectra*, **5**(1): 153–174.

FEMA-273 (1997), *NEHRP Guidelines for the Seismic Rehabilitation of Buildings*, FEMA Publication 273, Washington, DC: Federal Emergency Management Agency, October.

FEMA-356 (2000), *NEHRP Guidelines for the Seismic Rehabilitation of Buildings*, FEMA Publication 356, Washington, DC: Federal Emergency Management Agency, November.

Farahi M and Mofid M (2013), "On the Quantification of Seismic Performance Factors of Chevron Knee Bracings, in Steel Structures," *Engineering Structures*, **46**(1): 155–164.

Ghaffarzadeh H and Maheri MR (2006), "Mechanical Compression Release Device in Steel Bracing System for Retrofitting RC Frames," *Earthquake Engineering and Engineering Vibration*, **5**(1): 151–158. https://doi.org/10.1007/s11803-006-0626-x

Ghobarah A and Abou-Elfath H (2001), "Rehabilitation of a Reinforced Concrete Frame Using Eccentric Steel Bracing," *Engineering Structures*, **23**: 745–755.

Godínez-Domínguez EA and Tena-Colunga A (2010), "Nonlinear Behavior of Code-Designed Reinforced Concrete Concentric Braced Frames under Lateral Loading," *Engineering Structures*, **32**(4): 944–963.

Godínez-Domínguez EA, Tena-Colunga A and Pérez-Rocha LE (2012), "Case Studies on the Seismic Behavior of Reinforced Concrete Chevron Braced Framed Buildings," *Engineering Structures*, **45**: 78–103.

Godínez-Domínguez EA and Tena-Colunga A (2016), "Redundancy Factors for the Seismic Design of Ductile Reinforced Concrete Chevron Braced Frames," *Latin American Journal of Solids and Structures*, **13**(11): 2088–2112.

Hartzell SH (1978), "Earthquake Aftershocks as Green's Functions," *Geophysical Research Letters*, **5**: 1–4.

Henry RS, Sritharan S and Ingham JM (2016), "Residual Drift Analyses of Realistic Self-Centering Concrete Wall Systems," *Earthquakes and Structures*, **10**(2): 409–428.

Ikeda K, Mahin S and Dermitzakis S (1984), "Phenomenological Modeling of Steel Braces under Cyclic Loading," *Report No. UCB/EERC-84/09*, Department of Civil Engineering, University of California at Berkeley.

Ikeda K and Mahin S (1984), "A Refined Physical Theory for Predicting the Seismic Behavior of Braced Steel Frames," *Report No. UCB/EERC-84/12*, Department of Civil Engineering, University of California at Berkeley.

Ju M, Lee KS, Sim J and Kwon H (2014), "Non-Compression X-Bracing System Using CF Anchors for Seismic Strengthening of RC Structures," *Magazine of Concrete Research*, **66**(4): 159–174.

Kappos AJ (1999), "Evaluation of Behaviour Factors on the Basis of Ductility and Overstrength Studies," *Engineering Structures*, **21**(9): 823–835.

Kadid A and Yahiaoui D (2011), "Seismic Assessment of Braced RC Frames," *Procedia Engineering: The Proceedings of the Twelfth East Asia-Pacific Conference on Structural Engineering and Construction*, **14**: 2899–2905.

Kawamata S and Ohnuma M (1980), "Strengthening

Effect of Eccentric Steel Braces to Existing Reinforced Concrete Frames," *Proceedings, 7th World Conference on Earthquake Engineering*, Istanbul, Turkey.

Khatib I, Mahin S and Pister K (1988), "Seismic Behavior of Concentrically Braced Steel Frames," *Report No. UCB/EERC-88/01*, Earthquake Engineering Research Center, University of California at Berkeley.

Khampanit A, Leelataviwat S, Kochanin J and Warnitchai P (2014), "Energy-Based Seismic Strengthening Design of Non-Ductile Reinforced Concrete Frames Using Buckling-Restrained Braces," *Engineering Structures*, **81**: 110–122.

Kemp RA (1996), "Inelastic Local and Lateral Buckling in Design Codes," *ASCE Journal of Structural Engineering*, **122**(4): 374–382.

Liu F, Wang L and Lu X (2012), "Experimental Investigations on the Seismic Performance of Un-Retrofitted and Retrofitted RC Frames," *Proceedings, 15th World Conference on Earthquake Engineering*, Lisbon, Portugal.

Maheri MR and Sahebi A (1997), "Use of Steel Bracing in Reinforced Concrete Frames," *Engineering Structures*, **19**(12): 1018–1024.

Maheri MR and Akbari R (2003), "Seismic Behaviour Factor, R, for Steel *X*-Braced and Knee-Braced RC Buildings," *Engineering Structures*, **25**(12): 1505–1513.

Maheri MR, Kousari R and Razazan M (2003), "Pushover Tests on Steel *X*-Braced and Knee-Braced RC Frames," *Engineering Structures*, **25**(13): 1697–1705.

Maheri MR and Hadjipour A (2003), "Experimental Investigation and Design of Steel Brace Connection to RC Frame," *Engineering Structures*, **25**(13): 1707–1714.

Maheri MR and Ghaffarzadeh H (2008), "Connection Overstrength in Steel-Braced RC Frames," *Engineering Structures*, **30**(7): 1938–1948.

Maheri MR and Yazdani S (2016), "Design of Steel Brace Connection to an RC Frame Using Uniform Force Method," *Journal of Constructional Steel Research*, **116**: 131–140.

Martínez-Romero E (1993), "Experiences on the Use of Supplementary Energy Dissipators on Building Structures," *Earthquake Spectra*, **9**(3): 581–626.

Masri A and Goel S (1996), "Seismic Design and Testing of an RC Slab-Column Frame Strengthened by Steel Bracing," *Earthquake Spectra*, **12**(4): 645–666.

Newmark NM and Hall WJ (1982), *Earthquake Spectra and Design*, Monograph series, Earthquake Engineering Research Institute, Oakland.

Mitchell D and Paultre P (1994), "Ductility and Overstrength in Seismic Design of Reinforced Concrete Structures," *Canadian Journal of Civil Engineering*, **21**(6): 1049–1060.

MOC-15 (2015), *Manual de diseño de obras civiles, diseño por sismo*, Comisión Federal de Electricidad, México. (in Spanish)

Nateghi-A F (1995), "Seismic Strengthening of Eight-Storey RC Apartment Building Using Steel Braces," *Engineering Structures*, **17**(6): 455–461.

MFDC-04 (2004), *Reglamento de Construcciones para el Distrito Federa*, Gaceta Oficial del Departamento del Distrito Federal. (in Spanish)

NTCC-2004 (2004), *Normas Técnicas Complementarias para Diseño y Construcción de Estructuras de Concreto*, Gaceta Oficial del Distrito Federal, October. (in Spanish)

NTCS-2004 (2004), *Normas Técnicas Complementarias para Diseño por Sismo*, Gaceta Oficial del Distrito Federal, Tomo II, No. 103-BIS, 55-77, October. (in Spanish)

Osman A, Rashed A and El-Kady M (2006), "Seismic Response of RC Frames with Concentric Steel Bracing," *Proceedings, 8th National Conference on Earthquake Engineering*, San Francisco, California, CDROM, Paper No. 1979.

Park R, Priestley MJN and Gill WD (1982), "Ductility of Square-Confined Concrete Columns," *ASCE Journal of Structural Engineering*, **108**(4): 929–950.

Pérez-Rocha LE (1998), "Respuesta Sísmica Estructural: Efectos de Sitio e Interacción Suelo-Estructura (Aplicaciones al Valle de México)," *PhD Thesis*, División de Estudios de Posgrado de la Facultad de Ingeniería, Universidad Nacional Autónoma de México. (in Spanish)

Qiao S, Han X and Zhou K (2017), "Bracing Configuration and Seismic Performance of Reinforced Concrete Frame with Brace," *The Structural Design of Tall and Special Buildings*, **26**(e1381): 1–14.

Qu Z, Xie J, Wang T and Kishiki S (2017), "Cyclic Loading Test of Double K-Braced Reinforce Concrete Frame Subassemblies with Buckling Restrained Braces," *Engineering Structures*, **139**(15):1–14.

Remennikov AM and Walpole WR (1995), "Incremental Model for Predicting the Inelastic Hysteretic Behaviour of Steel Bracing Members," *Research Report 95-6*, Department of Civil Engineering, University of Canterbury, Christchurch, New Zealand.

Remennikov A and Walpole W (1997a), "Modelling the Inelastic Cyclic Behaviour of a Bracing Member for Work-Hardening Material," *International Journal of Solids and Structures*, **34**(27): 3491–3515.

Remennikov A and Walpole W (1997b), "Analytical Prediction of Seismic Behaviour for Concentrically-Braced Steel Systems," *Earthquake Engineering and Structural Dynamics*, **26**(8): 859–874.

Ruiz J and Miranda E (2006), "Evaluation of Residual Drift Demands in Regular Multi-Storey Frames for Performance-Based Seismic Assessment," *Earthquake Engineering and Structural Dynamics*, **35**(13): 1609–1629.

Saiidi M and Sozen MA (1979), "Simple and Complex Models for Nonlinear Seismic Response of Reinforced

Concrete Structures," *Structural Research Series No. 465*, Department of Civil Engineering, University of Illinois at Urbana-Champaign, August.

Sharmaa A, Eligehausen R and Reddya GR (2011), "A New Model to Simulate Joint Shear Behavior of Poorly Detailed Beam–Column Connections in RC Structures under Seismic Loads, Part I: Exterior Joints," *Engineering Structures*, **33**: 1034–1051.

Tagawa Y, Aoki H, Huang T and Masuda H (1992), "Experimental Study of New Seismic Strengthening Method for Existing RC Structure," *Proceedings, Tenth World Conference on Earthquake Engineering*, Rotterdam, 5193–5198.

Tapia-Hernández E and Tena-Colunga A (2014), "Code-Oriented Methodology for the Seismic Design of Regular Steel Moment Resisting Braced Frames," *Earthquake Spectra*, **30**(4): 1683–1709.

Tena-Colunga A, Del Valle E and Pérez-Moreno D (1996), "Issues on the Seismic Retrofit of a Building Near Resonant Response and Structural Pounding," *Earthquake Spectra*, **12**(3): 567–597.

Tena-Colunga A (1999), "International Seismic Zone Tabulation Proposed by the 1997 UBC Code: Observations for Mexico," *Earthquake Spectra*, **15**(2): 331–360.

Tena-Colunga A (2007), "State of the Art and State of the Practice for Energy Dissipation and Seismic Isolation of Structures in Mexico," *Proceedings, 10th World Conference on Seismic Isolation, Energy Dissipation and Active Vibration Control of Structures*, Istanbul, Turkey, CD-ROM.

Tena-Colunga A, Godínez-Domínguez EA and Pérez-Rocha, LE (2007), "Vulnerability Maps for Reinforced Concrete Structures for Mexico City's Metropolitan Area under a Design Earthquake Scenario," *Earthquake Spectra*, **23**(4): 809–840.

Tena-Colunga A, Correa-Arizmendi H, Luna-Arroyo JL and Gatica-Avilés G (2008), "Seismic Behavior of Code-Designed Medium Rise Special Moment-Resisting Frame RC Buildings in Soft Soils of Mexico City," *Engineering Structures*, **30**(12): 3681–3707.

Tena-Colunga A, Mena-Hernández U, Pérez-Rocha LE, Avilés J, Ordaz M and Vilar JI (2009), "Updated Seismic Design Guidelines for Buildings of a Model Code of Mexico," *Earthquake Spectra*, **25** (4): 869–898.

Tena-Colunga A and Cortés-Benítez JA (2015), "Assessment of Redundancy Factors for the Seismic Design of Special Moment Resisting Reinforced Concrete Frames," *Latin American Journal of Solids and Structures*, **12**(12): 2330–2350.

Tena-Colunga A and Nangullasmú-Hernández HJ (2015), "Assessment of Seismic Design Parameters of Moment Resisting RC Braced Frames with Metallic Fuses," *Engineering Structures*, **95**: 138–153.

Tena-Colunga A and Hernández-Ramírez H (2017), "Code-Oriented Global Design Parameters for Moment-Resisting Steel Frames with Metallic Structural Fuses," *Frontiers in Built Environment*, **3**(19): 1–16.

Tong GS, Luo GF and Zhang L (2012), "Lateral Resistance of Moment Resisting-Chevron Braced Frames with Weak Beams," *Harbin Gongye Daxue Xuebao/Journal of Harbin Institute of Technology*, **44**(10): 128–134.

Uriz P, Filippou FC and Mahin SA (2008), "Model for Cyclic Inelastic Buckling of Steel Braces," *Journal of Structural Engineering-ASCE*, **134**(4): 619–628.

Vona M and Mastroberti M (2018), "Estimation of the Behavior Factor of Existing RC-MRF Buildings," *Earthquake Engineering and Engineering Vibration*, **17**(1): 191–204. https://doi.org/10.1007/s11803-018-0434-0

Xiao J, Li J and Chen J (2011), "Experimental Study on the Seismic Response of Braced Reinforced Concrete Frame with Irregular Columns," *Earthquake Engineering and Engineering Vibration*, **10**(4): 487–494. https://doi.org/10.1007/s11803-011-0083-z.

Youssef MA, Ghaffarzadeh H and Nehdi M (2007), "Seismic Performance of RC Frames with Concentric Internal Steel Bracing," *Engineering Structures*, **29**(7): 1561–1568.

Zhang L, Luo GF and Tong GS (2013), "Refined Study on Lateral-Force Resistance of Dual Structural System Composed of Moment-Resisting Frame and Chevron Braces," *Journal of Zhejiang University* (*Engineering Science*), **47**(10): 1815–1823.